https://doi.org/10.1016/j.scitotenv.2017.06.161

Observation of SOA tracers at a mountainous site in Hong Kong: chemical characteristics, origins and implication on particle growth

X.P. Lyu [1], H. Guo [1*], H.R. Cheng [2**], X.M. Wang [3], X. Ding [3], H.X. Lu [1], D.W. Yao [1], and C. Xu [1]

[1] Department of Civil and Environmental Engineering, The Hong Kong Polytechnic University, Hong Kong

[2] Department of Environmental Engineering, School of Resource and Environmental Sciences, Wuhan University, Wuhan, China

[3] State Key Laboratory of Organic Geochemistry, Guangzhou Institute of Geochemistry, Chinese Academy of Sciences, Guangzhou, China

Corresponding author: H. Guo (ceguohai@polyu.edu.hk); H.R. Cheng (chenghr@whu.edu.cn)

Abstract: Secondary organic aerosol (SOA) is an important constituent of airborne fine particles. $PM_{2.5}$ (particles with aerodynamic diameters ≤ 2.5 μm) samples were collected at a mountainous site in Hong Kong in autumn of 2010, and analyzed for SOA tracers. Results indicated that the concentrations of isoprene SOA tracers (54.7±22.7 ng/m^3) and aromatics SOA tracers (2.1±1.6 ng/m^3) were on relatively high levels in Hong Kong. Secondary organic carbon (SOC) derived from isoprene, monoterpenes, sesquiterpenes and aromatics was estimated with the SOA tracer based approach, which constituted 0.35±0.15 μg/m^3 (40.6±5.7%), 0.20±0.03 μg/m^3 (30.4±5.5%), 0.05±0.02 μg/m^3 (5.6±1.7%) and 0.26±0.20 μg/m^3 (21.3±8.2%) of the total estimated SOC. Biogenic SOC (0.60±0.18 μg/m^3) dominated over anthropogenic SOC (0.26±0.20 μg/m^3) at this site. In addition to the total estimated SOC (17.8±4.6% of organic carbon (OC) in $PM_{2.5}$), primary organic carbon (POC) emitted from biomass burning also accounted for a considerable proportion of OC (11.6±3.2%). Insight into the OC origins found that regional transport significantly (p<0.05) elevated SOC from 0.37±0.17 to 1.04±0.39 μg/m^3. Besides, SOC load could also increase significantly if there was influence from local ship emission. Biomass burning related POC in regional air masses (0.81±0.24 μg/m^3) was also higher (p<0.05) than that in samples affected by local air (0.29±0.35 μg/m^3). Evidences indicated that SOA formation was closely related to new particle formation and the growth of nucleation mode particles, while biomass burning was responsible for some particle burst events in Hong Kong. This is the first SOA study in afforested areas of Hong Kong.

Keywords: Secondary organic aerosol, SOA tracer, biogenic SOA, regional transport, particle growth

1. Introduction

Atmospheric aerosol has been well recognized to affect global climate change (Stocker et al, 2013), human health (Dockery et al., 1993; Pope III and Dockery, 2006), visibility (Appel et al., 1985) and sustainability of economy (Chameides et al., 1999). Secondary organic aerosol (SOA) has been identified to play critical roles in these effects (Maria et al., 2004; Volkamer et al., 2006; Baltensperger et al., 2008), thus receiving sufficient attentions in recent years.

So far, the scientific community has reached a consensus that volatile organic compounds (VOCs) from biogenic emissions and anthropogenic aromatics are key precursors of SOA (Forstner et al., 1997; Claeys, et al., 2004). In global scale, biogenic SOA is thought to be the greatest constituent of SOA, due to the worldwide largest emission of biogenic VOCs (*e.g.*, isoprene, monoterpenes and sesquiterpenes) and formation of biogenic SOA spanning a wide range of conditions (the level of NO_x, humidity and aerosol acidity) (Kroll et al., 2006). However, anthropogenic SOA has also been found to be significant in urban areas (Volkamer et al., 2006). Furthermore, upon the findings that biogenic SOA correlates well with the indicators of anthropogenic emissions (Goldstein et al., 2009; Hoyle et al., 2011), it is believed that man-made air pollutants promote the formation of biogenic SOA, in addition to serving as SOA precursors themselves. These promoting effects at least include forming aerosol seeds, catalyzing photooxidation and transformation of biogenic VOCs and their oxidation products and changing the reaction pathways (*e.g.*, atmospheric fate of isoprene in low- and high-NO_x environments) (Hoyle et al., 2011). It is believed that SOA is a collection of hundreds to thousands of organic chemicals featuring relatively low volatilities. To understand SOA formation and explore the potential sources, SOA speciation is of great necessity. However, due to the difficulty in chemical analysis of SOA tracers, the chemical compositions of SOA are far from being well understood. The traditional analysis by gas chromatography-mass spectrometer detector (GC-MSD) generally quantifies a total of less than 20 organic compounds in particles (Offenberg et al., 2007; Kleindienst et al., 2007). Although some advanced instruments have been developed nowadays, such as aerosol mass spectrometry and thermal desorption aerosol gas chromatography, they are either fragment-based or highly dependent upon the skills and knowledge of users (Williams et

al., 2014). Instead, SOA tracer based approach is a simplified method widely used to estimate the amount, precursors and sources of SOA (Kleindienst et al., 2007; Ding et al., 2012).

The SOA tracer based approach applies the laboratory obtained ratios between the sum of specific SOA tracers and total mass of SOA (or secondary organic carbon (SOC)) produced from individual (group of) species to the field measured SOA tracers (Kleindienst et al., 2007), roughly estimating SOA (SOC) derived from an individual VOC or VOC group. Table S1 summarizes the VOC precursors, corresponding SOA tracers and the ratios between SOA tracers and SOA (or SOC), as reported by Kleindienst et al. (2007). The drawbacks of this method are obvious. For instance, it is controversial whether the laboratory obtained ratios can be directly applied to the field measured SOA tracers. However, it provides a feasible approach to estimate the SOA concentration, which is especially helpful in the cases of not well knowing the SOA compositions. More importantly, Offenberg et al. (2007) confirmed that the SOA tracer based approach was reliable through comparing with the results obtained from ^{14}C contents.

Hong Kong, one of the most developed regions in East Asia, has a total territory area of ~1.1×10^3 km^2 and a total population of ~7 million. Despite high population density, it keeps 24 country parks and a vegetation coverage rate of 70%. Evergreen broadleaf trees are common in Hong Kong. Guenther et al. (2006) suggested that shrubs are large emitters of isoprene, a typical and most abundant biogenic VOC. The total emission amount of biogenic VOCs in Hong Kong is estimated as 8.6×10^3 ton C/a (Tsui et al., 2009). Field measurements also revealed that isoprene in Hong Kong is relatively high (300-400 pptv) (Guo et al., 2007, 2012a). In contrast, aromatics are largely emitted from vehicular exhaust and solvent usage in Hong Kong. For example, toluene is one of the most abundant aromatics, with the level of 3-6 ppbv (Guo et al., 2004; Ho et al., 2004). Therefore, local emission of VOCs has a great potential forming SOA in Hong Kong. In addition to local SOA formation, regional transport is inevitable due to severe air pollution in upwind direction of Hong Kong (*i.e.*, inland Pearl River Delta (PRD) region). Studies confirmed that Hong Kong received SOA produced by isoprene and toluene from inland PRD region (Hu et al., 2008). However, the previous SOA studies in Hong Kong all focused on urban areas, which are not enough to understand the abundance, compositions and sources of SOA in low-altitude mountainous area where both anthropogenic and biogenic emissions are important.

In this study, SOC derived from isoprene, monoterpenes, sesquiterpenes and aromatics at a mountainous site in Hong Kong were estimated using a SOA tracer based approach. Local and regional contributions to SOC and biomass burning related POC were determined. Furthermore, in combination with particle size distribution simultaneously monitored by a scanning mobility particle sizer (SMPS), the relationships between SOA formation and particle growth were examined.

2. Methodology

2.1 Sample collection

Hong Kong, a coastal city surrounded by the South China Sea (SCS) to the east and south, is located in southern China. Under the dominance of subtropical monsoon climate, Hong Kong receives northerly winds originating from the heavily polluted PRD region in cool seasons (October-March), while prevailing southerly winds bring in clean air from SCS in warm seasons (April-August) (So and Wang, 2003). The sampling site (22.405° N, 114.118° E, 640 m a.s.l) was set up at the mountainside of the highest mountain in Hong Kong (Mt. Tai Mo Shan with the maximum altitude of 957 m, TMS). The vegetation on this mountain mainly includes Acacia confusa, Lophotemon confertus, Machilus chekiangensis and Schima superba below 550 m, while it turns to shrubs and grasses above 550 m (Guo et al., 2012b). As demonstrated in previous studies (Guo et al., 2013; Ling et al., 2014), regional transport of air pollutants from inland PRD, mesoscale circulation (mountain-valley breezes) and in situ atmospheric chemistry are the main processes that significantly influence air quality at this site. Figure 1 shows the geographical locations of the sampling site and air quality monitoring stations (AQMSs) of Hong Kong Environmental Protection Department (HKEPD).

From September 7 to November 26, 2010, a total of 19 $PM_{2.5}$ samples were collected. The instrument was an Anderson high volume $PM_{2.5}$ sampler, with a flow rate of 750 L/min. Pre-baked A4 size quartz fiber filters were used to collect the samples, which were stored in the refrigerator at -18 °C after sampling. Generally, each filter sampling lasted for 45-55 hours, except for the cases that the instrument stopped abnormally on some days due to thunderstorm-caused power outages. Table S2 lists the sample IDs, start and end dates & times. The origins of air masses, as distinguished by wind field and ratio of SO_2/NO_x (see section 3.3 for details), are also shown in the table. Additionally, the particle number concentrations and size distributions in the size range of 5.5-350.4 nm in 44 size bins were monitored by a scanning mobility particle

sizer (SMPS) from October 27 to November 29. Detailed introductions about the operation procedures of SMPS and data processing can be found in Guo et al. (2012a). We also collected ambient VOC samples during September 28-November 21. Inorganic trace gases (SO_2, CO, NO, NO_2 and O_3) and weather conditions were measured simultaneously with the $PM_{2.5}$ sampling. Details about VOC sampling, VOC analysis and monitoring of trace gases are provided in Guo et al. (2013) and Ling et al. (2014).

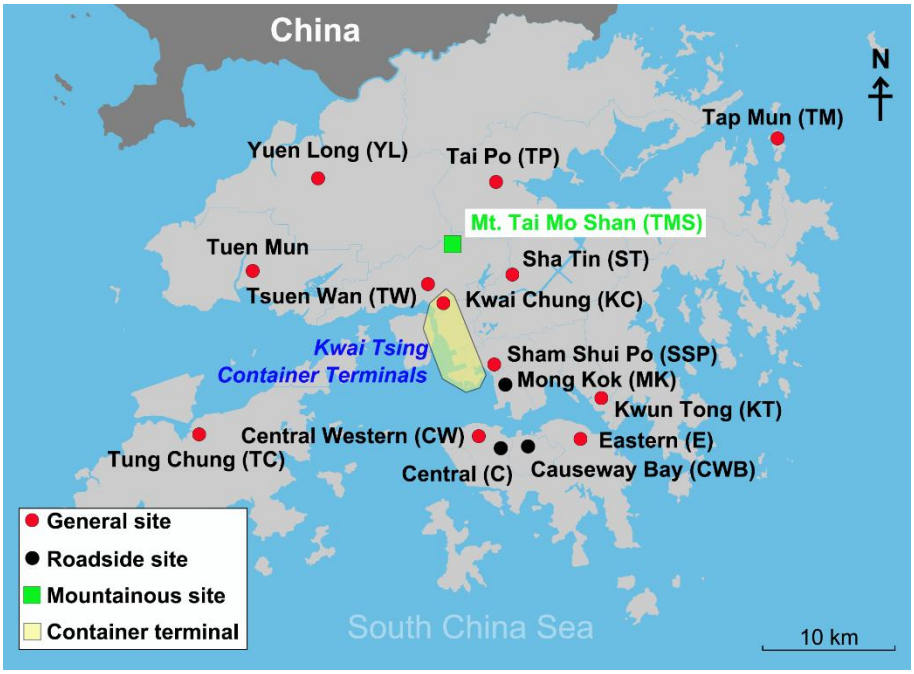

Figure 1 Geographic locations of the sampling site (TMS), AQMSs of HKEPD and the container terminal area where nine container terminals are located. Capital letters in the brackets are abbreviations of the site/stations

2.2 Chemical analysis

OC and element carbon (EC) in $PM_{2.5}$ samples were analyzed using the thermo-optical transmittance method recommended by National Institute for Occupational Safety and Health (NIOSH) (Birch, 1998). The concentrations of OC and EC are shown in Figure S1.

The method of SOA analysis was in line with that introduced by Ding et al. (2011). Briefly, the procedures for each sample include solvent extraction, derivation, analysis by GC-MSD, and identification and quantification of SOA tracers. 1/8 of each filter was extracted three times by sonication in the solvent of 40 mL of 1:1 (v/v) dichloride methane (DCM)/methanol mixture. Prior to extraction, the internal standards (hexadecanoic acid-D_{31}, phthalic acid-D_4 and

levoglucosan-$^{13}C_6$) were spiked into the samples. The three-time extracts of each sample were combined, filtered and concentrated to ~2 mL, which was further divided into two parts for methylation and silylation derivation, respectively. In methylation derivation, the extract experienced a gentle nitrogen blow to dryness, and subsequent addition of 200 μL of DCM, 10 μL of methanol and 300 μL of freshly prepared diazomethane. Then, it was kept in room temperature for one hour to derivatize acids to methyl esters, after which the sample was blown to 200 μL and used for analysis of some *α*-pinene SOA tracers (Pinonic acid, pinic acid and 3-methyl-1,2,3-butanetricarboxylic acid). The silylation reagent was 100 μL of pyridine and 200 μL of N,O-bis-(trimethylsilyl)-trifluoroacetamide (BSTFA) plus 1% trimethylchlorosilane (TMCS). Differently, the derivation was carried out in an oven at 70 °C for one hour. One *α*-pinene SOA tracer (3-hydroxyglutanic acid) and tracers for isoprene SOA, sesquiterpenes SOA, and toluene SOA were analyzed from the silylated sample. An Agilent 5973N GC/MSD was employed to do the analysis. The identification of SOA tracers was based on the comparison of mass spectra with previous studies, and their retention time in GC chromatogram with other known compounds as the references. Pinonic acid and pinic acid were quantified by authentic standards. However, due to lack of standards, other *α*-pinene SOA tracers, isoprene SOA tracers, *β*-Caryophyllenic acid and 2,3-dihydroxy-4-oxopentanoic acid were quantified using pinic acid (PA), erythritol, octadecanoic acid and azelaic acid, respectively. The detection limits (DLs) for pinonic acid, pinic acid, erythritol, octadecanoic acid and azelaic acid were 0.05, 0.07, 0.06, 0.09, and 0.11 ng/m^3, respectively. Levoglucosan was also quantified with the DL of 0.15 ng/m^3. The SOA tracers analyzed in this study are highlighted in Table S1.

2.3 Quality assurance and quality control

In this study, internal standards were not spiked on the filters before sampling, to avoid their influences on OC analysis. According to the saturation concentrations of SOA tracers calculated by Ding et al. (2016), SOA tracers analyzed in this study were of low volatilities, except for pinonic acid. Therefore, pinonic acid in airborne $PM_{2.5}$ might be underestimated due to the blow-off effect during sampling, which however should not be significant to other SOA tracers. Recovery target compounds were spiked in the samples before analysis of SOA tracers. The recovery rates were 104±2%, 68±13%, 62±14%, 78±10%, 81±9% and 87±4% for pinonic acid, pinic acid, erythritol, octadecanoic acid, azelaic acid and levoglucosan, respectively. Since

internal standards were added into the samples prior to analysis, we did not use the recovery rates to correct the concentrations of SOA tracers.

2.4 Processing of SMPS data

In this study, particles measured by SMPS were divided into nucleation (5.5-24.7 nm), Aitken (24.7-101.4 nm) and accumulation modes (101.4-350.4 nm). Geometric mean diameter (GMD) for nucleation mode particles (5.5-24.7 nm) was calculated using the following equations (Guo et al., 2012a).

$$\mathrm{GRs} = \frac{d_{GMD}}{d_t} \quad \text{(Equation (1))}$$

$$\mathrm{GMD} = e^{(\sum n_i ln^{d_i})/N} \quad \text{(Equation (2))}$$

$$\frac{d_N}{d_{log}{}_{D_p}} = \frac{\Delta N}{log_{D_p^2} - log_{D_p^1}} \quad \text{(Equation (3))}$$

where n_i is the particle number concentration in the i^{th} bin with upper diameter of d_i, N represents the total number concentration (cm^{-3}). ΔN is the particle number concentration in the size bin with upper and lower limit diameter of $D_p{}^2$ and $D_p{}^1$, respectively.

Condensation sink (CS), which describes the loss rate of vapor molecules and newly formed particles on the pre-existing aerosol particles, was calculated as follows (Kulmala et al., 2005):

$$\mathrm{CS} = 2\pi \mathrm{D} \int D_p \beta_m(D_p) n(D_p) dD_p = 2\pi \mathrm{D} \sum_i \beta_{mi} D_{pi} N_i \quad \text{(Equation (4))}$$

where D is the diffusion coefficient of the condensing vapor, β_m is the transitional regime correction factor, D_p denotes the particle diameter, n and N represent the particle numbers. β_{mi}, D_{pi} and N_i are the specific values for a given size bin (i). Growth factor calculated according to Laakso et al. (2004) was used to calibrate the dry particle size measured by SMPS.

3. Results and discussion

3.1 Concentrations of SOA tracers

Table 1 shows the average concentrations of SOA tracers derived from different precursors at TMS. Isoprene SOA tracers were the most abundant (54.7±22.7 ng/m^3), followed by the tracers generated from monoterpenes (26.3±4.5 ng/m^3), aromatics (2.1±1.6 ng/m^3) and sesquiterpenes (1.1±0.4 ng/m^3). Figure 2 compares the concentrations of SOA tracers between previous studies and the present study. The number and species of SOA tracers for the same precursor were the same. For the cases that total concentration of monoterpenes SOA tracers was given (*e.g.*, Offenberg et al., 2011), a factor was applied to the total concentration to roughly estimate the

sum of monoterpenes SOA tracers with the number and species identical to this study (see section S1 and Figure S2 in the Supplement). It was found that isoprene SOA tracers at TMS were on relatively high level (54.7±22.7 ng/m^3), comparable to or even higher than those detected in the forest (61.4±30.4 ng/m^3 in Kleindienst et al. (2007) and 39.0±17.2 ng/m^3 in Offenberg et al. (2011)). In fact, isoprene at TMS was relatively low (2-517 pptv), the high isoprene SOA tracers indicated that biogenic SOA formation at this site might be enhanced by anthropogenic emissions, *e.g.*, sufficient aerosol seeds from SO_2-related new particle formation (Guo et al., 2012a). Certainly, regional transport could also contribute to high isoprene SOA tracers, as reported by Hu et al. (2008). For the anthropogenic SOA, the tracer produced by aromatics (2,3-dihydroxy-4-oxopentanoic acid) was noticeable. Although the average 2,3-dihydroxy-4-oxopentanoic acid in this study (2.1±1.6 ng/m^3) was not significantly higher than that in other studies (p>0.05), its maximum value reached 13.5 ng/m^3. Given abundant aromatics in the atmosphere of Hong Kong and mesoscale circulations between TMS and the surrounding urban areas, local formation could be an important factor contributing to high aromatics SOA at TMS. Moreover, it was reported that 2,3-dihydroxy-4-oxopentanoic acid at an urban background site in inland PRD was very high (13.1 ng/m^3) (Ding et al., 2012). Hence, regional transport might be partially responsible for the relatively high aromatics SOA tracer in Hong Kong. SOA tracers derived from monoterpenes and sesquiterpenes were on moderate levels, compared to other studies.

3-Methyl-1,2,3-butanetricarboxylic acid and 3-hydroxyglutanic acid, formed from monoterpenes oxidation in the presence of NO_x (Claeys et al., 2007; Eddingsaas et al., 2012), dominated the measured monoterpenes SOA tracers, consistent with those at an urban background site in inland PRD (Ding et al., 2012). Pinonic acid and pinic acid, formed from OH oxidation of α-pinene in NO_x free environment or ozonolysis of α-pinene (Eddingsaas et al., 2012), were also higher than those in urban areas of Hong Kong (almost below DLs) (Hu et al., 2008). Since NO_x was at the magnitude of several ppbv, the higher pinonic acid and pinic acid were likely due to the higher O_3 (69.2±2.4 ppbv at TMS and 30.8±2.6 ppbv at the mountain foot) at this mountainous site. In addition, other tracers including 3-hydroxy-4,4-dimethylglutaric acid, 3-isopropylpentanedioic acid, 3-acetylpentanedioic acid and 3-acetylhexanedioic acid, which were not measured in this study, accounted for 46.9±4.0% of the total amount of tracers according to Kleindienst et al. (2007). Of the isoprene SOA tracers, 2-methylthreitol and 2-methylerythritol are representative

products formed through the photooxidation of isoprene hydroxyhydroperoxides and acid catalysis of epoxydiols of isoprene in low NO_x environment when RO_2 reacting with HO_2 dominated the loss of RO_2 (Claeys et al., 2004; Surratt et al., 2010). In this study, they accounted for 83.5±8.1% of the total isoprene tracers. However, NO_x was not low enough and RO_2 reacting with NO was the main sink of RO_2 (Ling et al., 2014), implying that other mechanisms might enhance the formation of 2-methyltetrols (sum of 2-methylthreitol and 2-methylerythritol) at this site, such as acid catalysis (Surratt et al., 2007).

Table 1 Average concentrations of SOA tracers derived from monoterpenes, isoprene, sesquiterpenes and aromatics (mean±95% confidence interval (C.I.)).

VOC precursor	SOA tracer	Concentration (ng/m^3)
Monoterpenes	Pinonic acid	1.2±0.4
	Pinic acid	2.0±0.6
	3-methyl-1,2,3-butanetricarboxylic acid	16.0±3.5
	3-hydroxyglutanic acid	7.1±2.7
	Sum 1	26.3±4.5
Isoprene	2-Methylthreitol	14.7±6.6
	2-Methylerythritol	31.2±13.1
	2-methylglyceric acid	5.2±3.1
	cis-2-Methyl-1,3,4-trihydroxy-1-butene	0.8±0.5
	trans-2-Methyl-1,3,4-trihydroxy-1-butene	2.0±1.3
	3-Methyl-2,3,4-trihydroxy-1-butene	0.7±0.3
	Sum 2	54.7±22.7
Sesquiterpenes	*β*-Caryophyllenic acid	1.1±0.4
Aromatics	2,3-Dihydroxy-4-oxopentanoic acid	2.1±1.6

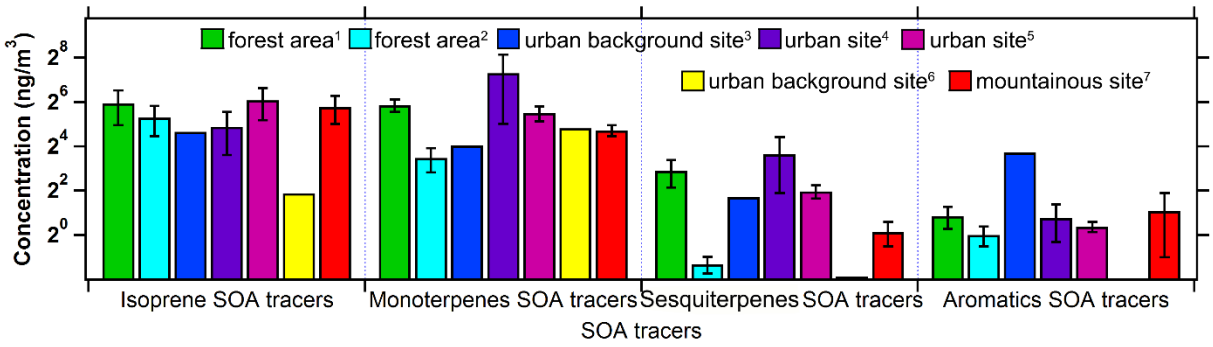

Figure 2 Comparison of SOA tracers between previous studies and this study. [1]Kleindienst et al. (2007); [2]Offenberg et al. (2011); [3]Ding et al. (2012); [4]Hu et al. (2008); [5]Lewandowski et al. (2008); [6]Haddad et al. (2011); [7]this study.

3.2 Estimate of SOC

Both the EC tracer method and SOA tracer method were used to estimate SOC (details about both methods are provided in section S2 of the Supplement). To apply the SOA tracer method, the sum of monoterpenes SOA tracers was scaled by a factor of 1.79 (see section S1 and Figure S2 for details). Figure S3 compares the SOC estimated by these two methods. SOC estimated by EC tracer method ($SOC_{EC\ tracer}$) were generally higher (p<0.01) than those estimated by SOA tracer method ($SOC_{SOA\ tracer}$), except for samples TMS1, TMS3 and TMS8. Ding et al. (2012) indicated that the EC tracer method might overestimate SOC, because it blended some primary OC (POC) from biomass burning with SOC. This inference was supported by the good correlation between the difference of SOC estimated by these two methods ($SOC_{EC\ tracer}$-$SOC_{SOA\ tracer}$) and levoglucosan, a tracer of biomass burning.

In addition to levoglucosan, methyl chloride (CH_3Cl) is an indicator of biomass burning (Rudolph et al., 1995). Figure 3 plots the correlation between levoglucosan and CH_3Cl at TMS, as well as that between $SOC_{EC\ tracer}$-$SOC_{SOA\ tracer}$ and levoglucosan. As expected, levoglucosan fairly correlated with CH_3Cl (R^2=0.54), further confirming the reliability of levoglucosan as the tracer of biomass burning. Consistent with Ding et al. (2012), good correlation was found between $SOC_{EC\ tracer}$-$SOC_{SOA\ tracer}$ and levoglucosan (R^2=0.52). This verified that the EC tracer method overestimated SOC due to the interference of biomass burning. Exceptionally, $SOC_{EC\ tracer}$ was remarkably lower than $SOC_{SOA\ tracer}$ for the samples TMS1, TMS3 and TMS8 (p<0.05). Further investigation found that on the sampling days of TMS1 and TMS3, the daily maximum hourly O_3 mixing ratio, referred to as peak O_3, was extremely high, with the values being the

second (154.4 ppbv) and first (163.4 ppbv) highest among the 19 filter samples, respectively, while during the sampling period of TMS8, the peak O_3 also reached 94.8 ppbv. In contrast, the average of peak O_3 values on the sampling days of other $PM_{2.5}$ filter samples was only 77.6 ppbv. Since high O_3 levels generally imply strong photochemical reactivity, high productions of SOA are also expected on these days. Hence, the higher $SOC_{SOA\ tracer}$ values observed in TMS1, TMS3 and TMS8 were understandable. We also found that there was no correlation between $SOC_{EC\ tracer}$ and peak O_3 (not shown), whereas $SOC_{SOA\ tracer}$ correlated well with peak O_3 (R^2=0.68), as shown in Figure 4, implying that the formation of secondary products, *i.e.*, SOA and O_3, depends upon the oxidative capacity of the atmosphere and they may also influence each other. Therefore, the SOA tracer method was believed to be more reliable and thus adopted in this study. Hereafter, SOC refers to $SOC_{SOA\ tracer}$, unless otherwise specified.

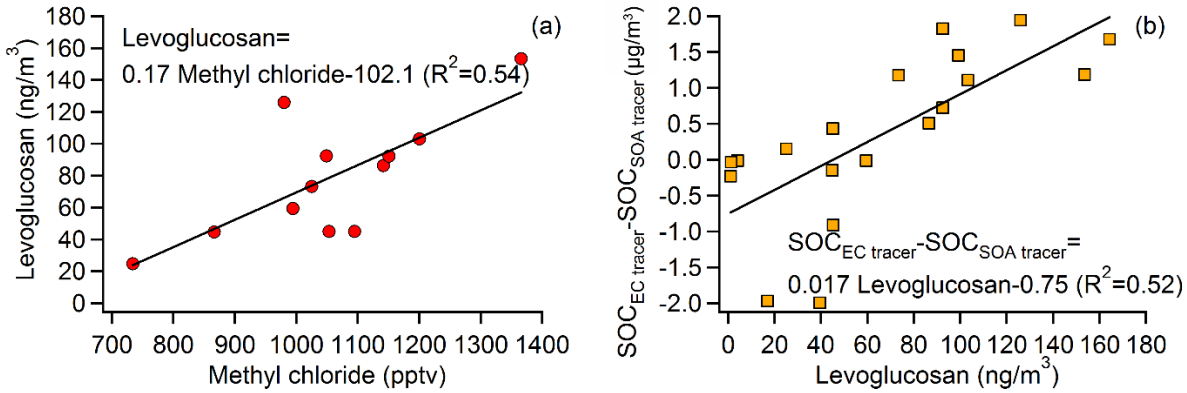

Figure 3 Linear correlations between (a) levoglucosan and CH_3Cl, and (b) $SOC_{EC\ tracer}$-$SOC_{SOA\ tracer}$ and levoglucosan.

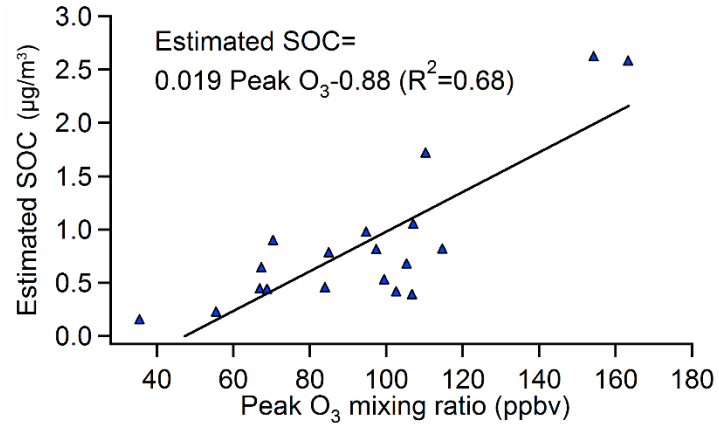

Figure 4 Linear correlation between $SOC_{SOA\ tracer}$ and peak O_3.

Figure 5 shows SOC produced by different groups of VOCs estimated using the SOA tracer based approach, and biomass burning related POC (POC $_{\text{biomass burning}}$). POC $_{\text{biomass burning}}$ was estimated by 0.01 (μg/ng) × levoglucosan (ng/m^3) (Lee et al., 2008). On average, SOC and POC $_{\text{biomass burning}}$ constituted 0.86±0.31 μg/m^3 (17.8±4.6%) and 0.67±0.22 μg/m^3 (11.6±3.2%) of OC (provided in Figure S1), respectively. The rest of OC were undetermined due to unknown sources and precursors of OC. The total SOC comprised anthropogenic (*i.e.*, aromatics) and biogenic (*i.e.*, isoprene, monoterpenes and sesquiterpenes) SOC, with the fractions of 21.3±8.2% (0.26±0.20 μg/m^3) and 78.7±8.2% (0.60±0.18 μg/m^3), respectively. Although anthropogenic SOC (ASOC) was significantly lower than biogenic SOC (BSOC) (p<0.05), ASOC had its highest value of 1.71 μg/m^3 in the sample TMS1, and BSOC reached its maximum in sample TMS3 (2.03 μg/m^3). As mentioned earlier, the two samples were collected on the days with very high O_3, indicating that aromatics and biogenic VOCs might be responsible for the high SOC in TMS1 and TMS3, respectively. However, VOC samples were not simultaneously collected during the collection of these two samples. Instead, the sample TMS12 was a good example because ASOC was the second highest (1.2 μg/m^3), and the daily average mixing ratio of toluene coincidently reached 4.0 ppbv during the TMS12 sampling period, the highest value among all VOC samples, which further confirmed the reliability of SOA tracer method in estimating SOC. Among SOC derived from biogenic VOCs, isoprene made the highest contribution (54.2±5.3% of BSOC and 42.7±5.9% of total SOC), followed by monoterpenes (37.9±4.6% and 30.4±5.5%, respectively) and sesquiterpenes (7.9±2.7% and 5.6±1.7%, respectively).

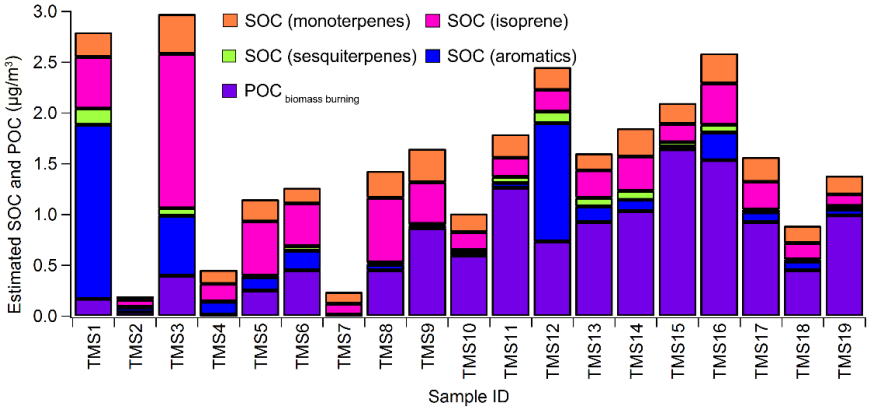

Figure 5 Concentrations of estimated SOC derived from monoterpenes, isoprene, sesquiterpenes and aromatics and POC $_{\text{biomass burning}}$.

3.3 Local and regional contributions to SOC

In line with the method used in Guo et al. (2013), the local and regional air masses were distinguished with the wind direction (WD) and wind speed (WS) monitored at TMS. Briefly, the northerly winds (0°<WD<90° or 270°<WD<360°) with WS higher than 2 m/s were considered to be capable of delivering air pollutants from the heavily polluted inland PRD region to the site. In these cases, the air masses were believed to be subject to regional influences. Otherwise, the site was dominated by local air. To validate this method, Figure 6 shows the hourly ratios of SO_2/NO_x for the air masses in different wind directions/speeds. Overall, the SO_2/NO_x ratios were higher for regional air masses, particularly when 0°<WD<90° and WS>2 m/s. This coincided with the lower sulfur content in vehicle fuels and higher vehicle emissions of NO_x in Hong Kong (Wang and So, 2003; Guo et al., 2009). For the 24-48 hr $PM_{2.5}$ samples (*i.e.*, duration of 1-2 days), the regional influence was not unexpected given that the northerly wind was stronger than 2 m/s for at least one hour on each sampling day. It was noteworthy that during the sampling periods of TMS1 and TMS16 (influenced by regional air), SO_2 was exclusively high at the HKEPD AQMSs in vicinity of the ship container terminals, *e.g.*, KC, SSP and TW (see Figure 1). Figure S4 presents SO_2 distributions at 14 AQMSs in Hong Kong during these two periods. In view of the fact that ship is a significant emitter of SO_2, the influence of local ship emission was also suspected for the two samples. According to these inferences, Table S2 lists the categories of the samples affected by regional air, local air, and local ship emissions, respectively.

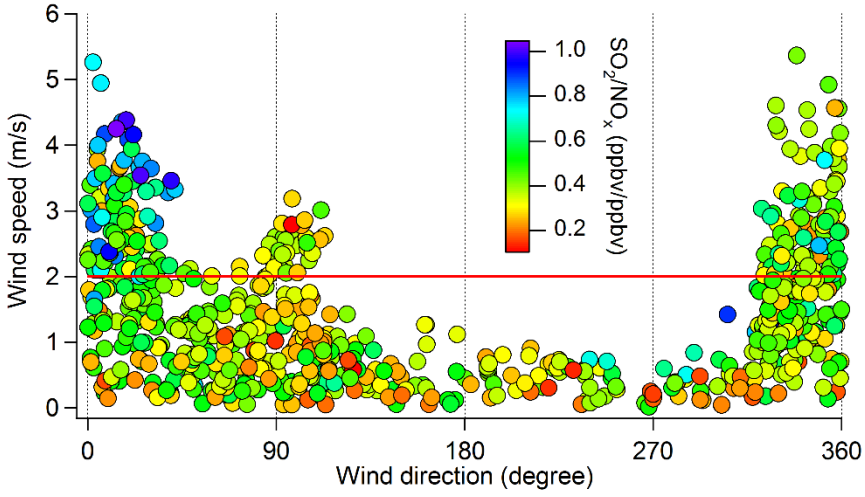

Figure 6 Hourly ratios of SO_2/NO_x for the air masses in different wind directions/speeds at TMS.

Table 2 summarizes the concentrations of SOC and $POC_{\text{biomass burning}}$ in different categories of air masses. Note that since the samples TMS1 and TMS16 were influenced by both regional air and local ship emission, they were separately discussed later. It was found that SOC derived from

individual group/species and total SOC in regional air were all significantly (p<0.05) higher than that in local air, suggesting that SOC at TMS was elevated by regional transport. Despite possible influences of local ship emissions in TMS1 and TMS16, the concentrations of SOC and POC in these two samples were well within the ranges of those in regional air, except for aromatics SOC (1.71 μg/m^3) in sample TMS1. The extremely high aromatics SOC in TMS1 might be caused by ship emissions which could be laden with high concentrations of aromatics. Contradictorily, SOC derived from aromatics was remarkably lower in TMS16 (0.27 μg/m^3). This discrepancy might be explained by the differences of fuel types and operating conditions of the ship engines, which were repeatedly proved to affect the emission characteristics of ship engines (Reda et al., 2014; Sippula et al., 2014). Similar to SOC, POC also showed a significantly higher level in regional air (0.81±0.24 μg/m^3) than that in local air (0.29±0.35 μg/m^3) (p<0.05). Since the high concentration of $POC_{biomass\ burning}$ in regional air was partially contributed by TMS16 ($POC_{biomass\ burning}$ =1.54 μg/m^3), a sample jointly influenced by regional air and local ship emission, specific insight was given to this sample. Firstly, ship emission was not likely to be the culprit of high $POC_{biomass\ burning}$, as no study reported ship emission of levoglucosan, the biomass burning tracer used to calculate $POC_{biomass\ burning}$ in this study. Instead, we found that another sample under the influence of regional air (TMS15) had comparable $POC_{biomass\ burning}$ (1.64 μg/m^3). Furthermore, CH_3Cl, another tracer of biomass burning, increased noticeably under northerly winds in sample TMS16, indicating the regional transport of biomass burning plumes into Hong Kong. In fact, nearly no fire spot in local Hong Kong was observed by the satellite during the sampling, compared to some open fires detected in upwind directions (see Figure S5). Therefore, $POC_{biomass\ burning}$ in TMS16 was reasonably speculated to be elevated by regional biomass burning plumes. Upon this inference, we concluded that regional transport significantly contributed to $PM_{2.5}$-bounded POC in Hong Kong.

Table 2 Mean±95% C.I. of SOC and POC in different categories of air masses (Unit: μg/m^3).

	Local air	Regional air	TMS1*	TMS16*
SOC (monoterpenes)	0.13±0.06	0.23±0.03	0.23	0.28
SOC (isoprene)	0.16±0.07	0.42±0.18	0.51	0.41
SOC (sesquiterpenes)	0.01±0.01	0.06±0.02	0.16	0.07
SOC (aromatics)	0.07±0.04	0.33±0.26	1.71	0.27

$POC_{biomass\ burning}$	0.29±0.35	0.81±0.24	0.17	1.54
Total SOC	0.37±0.17	1.04±0.39	2.61	1.04

* 95% C.I. is not available for a single sample.

3.4 Implications to particle formation and growth

As an important constituent of airborne particles, SOA plays critical role in particle formation and growth (Jang et al., 2003). The relationships between SOA formation and particle formation/growth were investigated on three selected days (October 31, November 09 and November 19) when SOC were among the highest of all the samples and SMPS data were available. Figures 7-9 show the evolutions of particle numbers, GMD of nucleation mode particles, CS, the simulated sulfuric acid (SA) vapor, oxidized intermediates of aromatics (AOI), oxidized intermediates of biogenic VOCs (BOI), and the measured inorganic trace gases. Details about the modelling of SA vapor, AOI and BOI are provided in Section S3 and Table S3 in the Supplement. For convenience of analysis, the hourly mixing ratios of biogenic VOCs (BVOCs), aromatics and CH_3Cl are presented in Figure S6.

In Figures 7-8, the number concentration of nucleation mode particles (N_{nuc}) increased substantially in the morning of October 31 (11:00-12:00) and November 09 (10:00-11:00), followed by the increases of number of Aitken mode particles (N_{Ait}). Prior to the increases of N_{nuc}, the simulated SA vapor began to increase about 3 hours earlier. These were consistent with the findings in Guo et al. (2012a) who reported that the increase of N_{nuc} was caused by new particle formation (NPF) events occurred on both days, and SA vapor played important roles in NPF. However, we further found that the oxidation intermediates of BVOCs (*i.e.*, BOI) also increased slightly ahead of the rise of N_{nuc}, which might suggest that the oxidation of BVOCs also made some contributions to NPF. In fact, the involvement of BVOCs in NPF at this afforested site has been speculated by Guo et al. (2012a), which is confirmed with the aid of model simulations in this study.

Moreover, we noticed that the nucleation mode particles experienced obvious growth with the rate of 1.9 nm/h (15:00-16:00) and 1.4 nm/h (14:00-16:00) in the afternoon of October 31 and November 09, respectively. Both growths occurred under the conditions of high N_{Ait} and high CS, differing from NPF events. Meanwhile, O_3 was on high level, which meant strong oxidative capacity of the atmosphere. Correspondingly, the simulated SA vapor, AOI and BOI showed great increments simultaneously with or 1-2 hours earlier than the increase of GMD. It is

noteworthy that the significant increases of AOI and BOI were also attributable to the rapid increases of VOCs (see Figure S6), in addition to strong atmospheric oxidative capacity. This suggested that the photo-oxidation of VOCs also facilitated the growth of nucleation mode particles. The prompt responses of particle growth to the increments of oxidation products on October 31 (rather than 1.5 hours' delay on November 09) were likely caused by the much more abundant BOI (~22.7 pptv) than that on November 09 (~13.5 pptv). Besides, the lower initial GMD before its increase on October 31 (~14 nm compared to ~16 nm on November 09) implied higher surface area and subsequently quicker growth. Since the aforementioned days featured high SOA, the roles of photo-oxidation of VOCs in the formation and growth of nucleation mode particles might reflect the very initial stages of SOA formation. However, to better understand the relationships between SOA formation and the formation/growth of particles, data with higher resolution and more comprehensive chemical information of SOA are crucially needed.

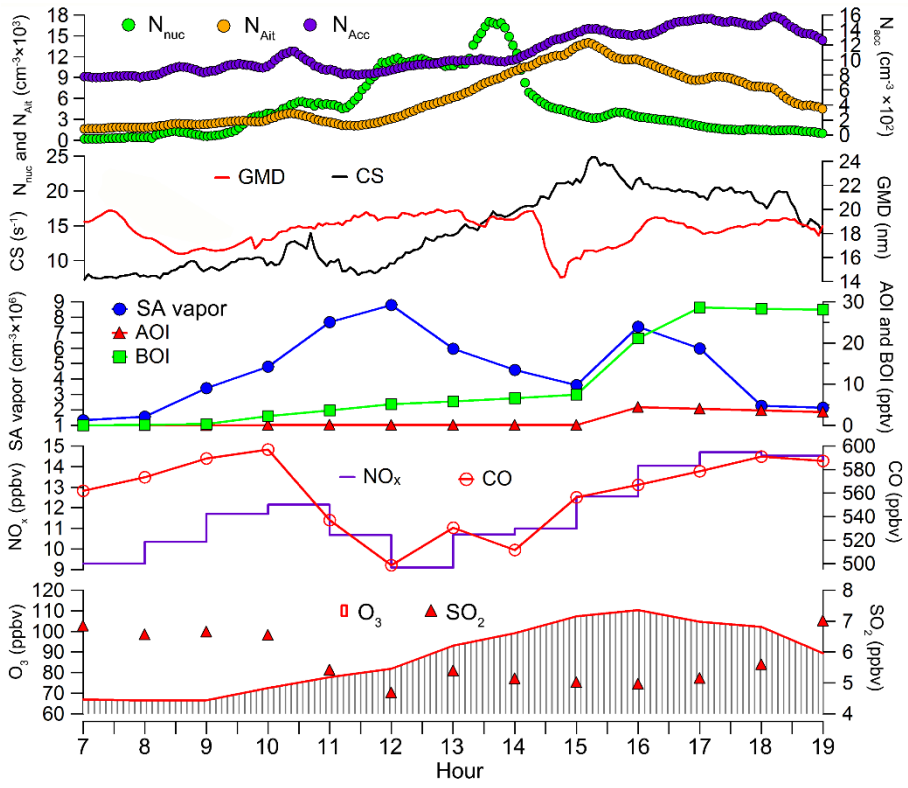

Figure 7 Evolutions of particle numbers, GMD of nucleation mode particles, CS, simulated SA vapor, AOI, BOI and inorganic trace gases on October 31 (first sampling day of TMS12).

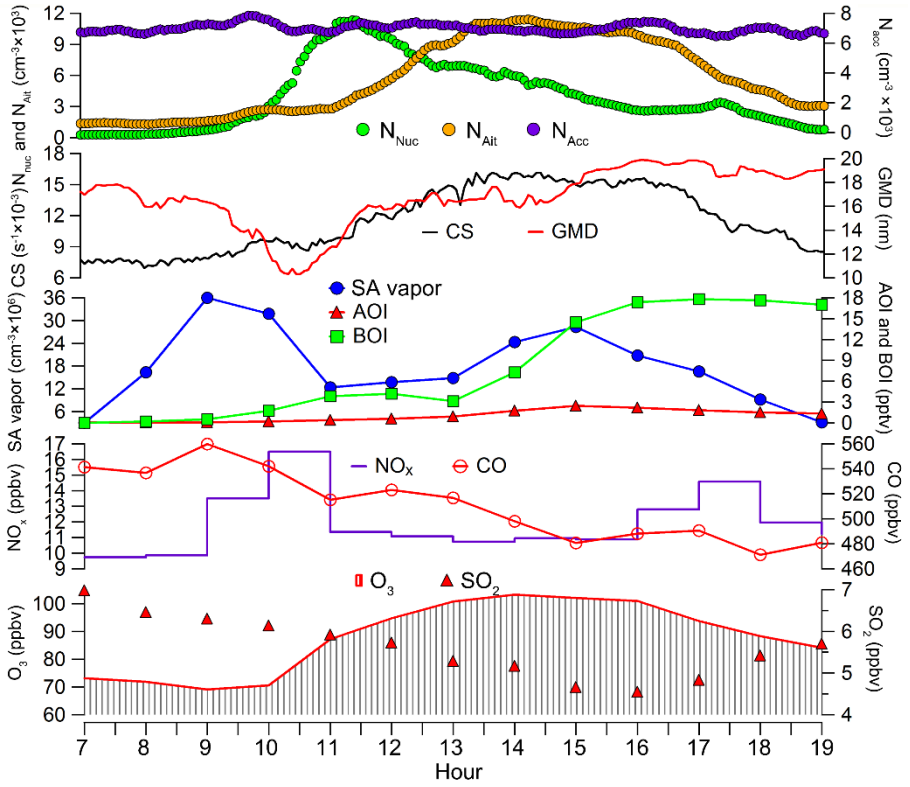

Figure 8 Evolutions of particle numbers, GMD of nucleation mode particles, CS, simulated SA vapor, AOI, BOI and inorganic trace gases on November 09 (second sampling day of TMS14).

Similarly, the growth of nucleation mode particles was also observed on November 19 (15:00-16:00) (Figure 9). However, a distinct phenomenon was that the numbers of particles in nucleation, Aitken and accumulation modes all showed rapid increases simultaneously from around 14:30 and reached the highest values at ~15:00, which indicated that the particles in different modes shared a common source. Although SO_2 and the simulated SA vapor began to increase 1.5 hours earlier, this could not be a NPF event, as the increase of N_{Ait} had no delay (no banana shape) and the CS was high. In addition, the levels of primary air pollutants (*e.g.*, NO_x and CO) were high at the peak hours of all three-mode particle numbers. More importantly, we found that CH_3Cl largely increased from 13:00 to 15:00 and reached the maximum at 15:00 (see Figure S6). Therefore, we suspected that biomass burning might be responsible for the increase of particle numbers. This coincided with the high $POC_{\text{biomass burning}}$ (1.54 μg/m^3) in $PM_{2.5}$ sample collected on this day (TMS16). Generally, particles emitted from biomass burning are in Aitken and accumulation modes (Reid et al., 2005). However, in vicinity of fire, nucleation mode can also exist (Janhall et al., 2010). Here, although nucleation mode particles increased in the particle

burst event, N_{nuc} was very low (maximum=2.1×10^3 cm^{-3}), indicating that this was not a local biomass burning and nucleation mode particles converted to larger size particles from the source region to this site. This was also consistent with the regional influence on this day identified by the wind fields (see section 3.3).

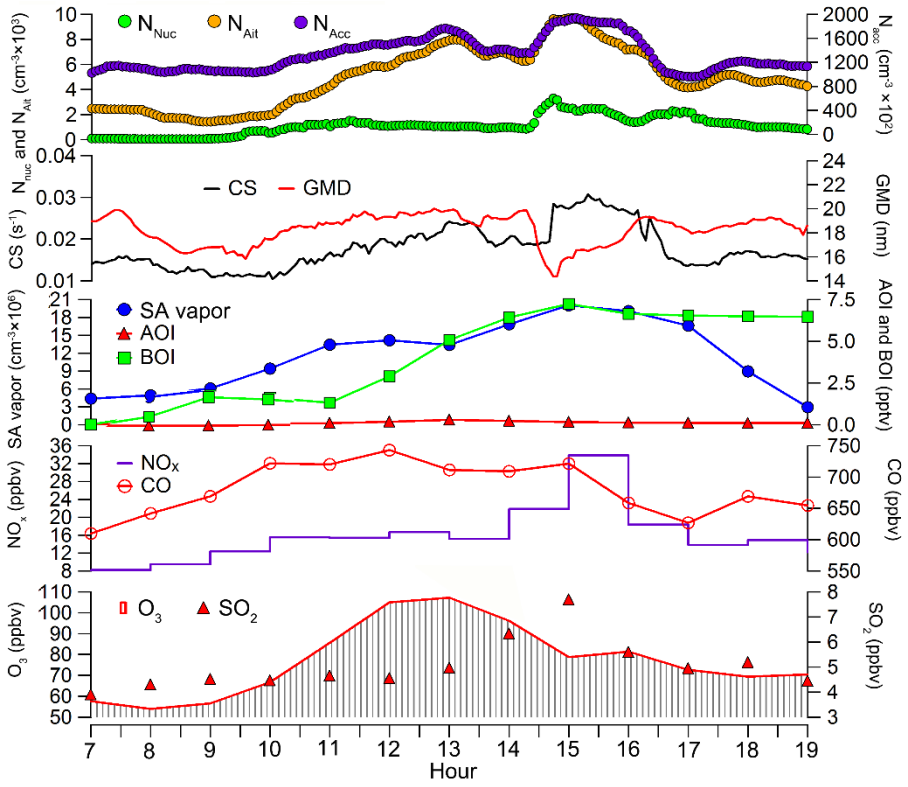

Figure 9 Evolutions of particle numbers, GMD of nucleation mode particles, CS, simulated SA vapor, AOI, BOI and inorganic trace gases on November 19 (sampling day of TMS16).

4. Conclusions

$PM_{2.5}$ samples were collected at a mountainous site in Hong Kong in autumn of 2010. Nine SOA tracers in $PM_{2.5}$ were analyzed, which helped to understand the compositions and sources of SOC in this study. Results indicated that isoprene made the highest contribution to SOC formation at this site, followed by monoterpenes, aromatics and sesquiterpenes. Averagely, biogenic SOC dominated over anthropogenic SOC. However, anthropogenic SOC cannot be neglected, particularly under the influences of regional transport (*e.g.*, 1.2 μg/m^3 in sample TMS12) and/or local ship emission (*e.g.*, 1.7 μg/m^3 in sample TMS1). The simultaneous observation of VOCs confirmed the role of aromatics in contributing to high concentrations of anthropogenic SOC. In terms of SOC origins, regional transport caused nearly two-fold increase

of SOC, relative to local air. However, SOC load could also be significantly elevated by local ship emissions possibly containing abundant VOC precursors and SO_2, which promoted SOC formation. In addition, the regional air was generally characterized with high biomass burning related POC, aggravating the $PM_{2.5}$-bounded POC in Hong Kong. In combination with the SMPS data, we found that the formation of SOA (particularly the biogenic SOA) might be partially responsible for the new particle formation and growth of nucleation mode particles. Primary emissions, such as biomass burning, could cause particle burst events and lead to POC increases. To our knowledge, this is the first SOA study carried out in low-altitude (640 m) mountainous area of Hong Kong, where the air quality is under the combined influence of anthropogenic and biogenic emissions. This study also demonstrates the urgency of data acquisition with more comprehensive chemical information and higher time resolution in future SOA studies over this region.

Acknowledgements

This study was supported by the Research Grants Council of the Hong Kong Special Administrative Region via grants CRF/C5004-15E, PolyU5154/13E, PolyU152052/14E, and CRF/C5022-14G, and the Hong Kong Polytechnic University PhD scholarships (project #RTUP). This study is partly supported by the Hong Kong PolyU internal grant (1-BBW4, 4-ZZFW, G-YBHT and 1-ZVJT) and by the Innovation and Technology Commission of the HKSAR via the Hong Kong Branch of National Rail Transit Electrification and Automation Engineering Technology Research Center (1-BBYD).

References

Appel, B.R., Tokiwa, Y., Hsu, J., Kothny, E.L., and Hahn, E., 1985. Visibility as related to atmospheric aerosol constituents. Atmos. Environ. (1967), 19(9), 1525-1534.

Birch, M.E., 1998. Analysis of carbonaceous aerosols: interlaboratory comparison. Analyst 123(5), 851-857.

Chameides, W.L., Yu, H., Liu, S.C., Bergin, M., Zhou, X., Mearns, L., Wang, G., Kiang, C.S., Saylor, R.D., Luo, C., Huang, Y., Steiner, A., and Giorgi, F., 1999. Case study of the effects of atmospheric aerosols and regional haze on agriculture: An opportunity to enhance crop yields in China through emission controls?. P. Natl. Acad. Sci. 96(24), 13626-13633.

Claeys, M., Graham, B., Vas, G., Wang, W., Vermeylen, R., Pashynska, V., Cafmeyer, J., Guyon, P., Andreae, M., Artaxo, P., and Maenhaut, W., 2004. Formation of secondary organic aerosols through photooxidation of isoprene. Science 303(5661), 1173-1176.

Claeys, M., Szmigielski, R., Kourtchev, I., Van der Veken, P., Vermeylen, R., Maenhaut, W., Jaoui, M., Kleindienst, T.E., Lewandowski, M., Offenberg, J.H. and Edney, E.O., 2007. Hydroxydicarboxylic acids: markers for secondary organic aerosol from the photooxidation of α-pinene. Environ. Sci. Technol. 41(5), 1628-1634.

Ding, X., Wang, X.M., Gao, B., Fu, X.X., He, Q.F., Zhao, X.Y., Yu, J.Z., and Zheng, M., 2012. Tracer-based estimation of secondary organic carbon in the Pearl River Delta, south China. J. Geophys. Res.: Atmos. 117(D5), doi: 10.1029/2011JD016596.

Ding, X., Zhang, Y.Q., He, Q.F., Yu, Q.Q., Shen, R.Q., Zhang, Y.L., Zhang, Z., Lyu, S.J., Hu, Q.H., Wang, Y.S., Li, L.F., Song, W., and Wang, X.M., 2016. Spatial and seasonal variations of secondary organic aerosol from terpenoids over China. J. Geophys. Res.: Atmos. 121, doi: 10.1002/2016JD025467.

Dockery, D.W., Pope, C.A., Xu, X., Spengler, J.D., Ware, J.H., Fay, M.E., Ferris Jr., B.G., and Speizer, F.E., 1993. An association between air pollution and mortality in six US cities. New Engl. J. Med. 329(24), 1753-1759.

Eddingsaas, N.C., Loza, C.L., Yee, L.D., Chan, M., Schilling, K.A., Chhabra, P.S., Seinfeld J.H., and Wennberg, P.O., 2012. α-pinene photooxidation under controlled chemical conditions-Part 2: SOA yield and composition in low-and high-NO_x environments. Atmos. Chem. Phys. 12(16), 7413-7427.

Forstner, H.J., Flagan, R.C., and Seinfeld, J.H., 1997. Secondary organic aerosol from the photooxidation of aromatic hydrocarbons: Molecular composition. Environ. Sci. Technol. 31(5), 1345-1358.

Goldstein, A.H., Koven, C.D., Heald, C.L., and Fung, I.Y., 2009. Biogenic carbon and anthropogenic pollutants combine to form a cooling haze over the southeastern United States. P. Natl. Acad. Sci. 106(22), 8835-8840.

Guo, H., Jiang, F., Cheng, H.R., Simpson, I.J., Wang, X.M., Ding, A.J., Wang, T.J., Saunders, S.M., Wang, T., Lam, S.H.M., Blake, D.R., Zhang, Y.L., and Xie, M., 2009. Concurrent observations of air pollutants at two sites in the Pearl River Delta and the implication of regional transport. Atmos. Chem. Phys. 9(19), 7343-7360.

Guo, H., Lee, S.C., Louie, P.K., Ho, K.F., 2004. Characterization of hydrocarbons, halocarbons and carbonyls in the atmosphere of Hong Kong. Chemosphere 57(10):1363-72.

Guo, H., Ling, Z.H., Cheung, K., Jiang, F., Wang, D.W., Simpson, I.J., Barletta, B., Meinardi, S., Wang, T.J., Saunders, S.M., and Blake, D.R., 2013. Characterization of photochemical pollution at different elevations in mountainous areas in Hong Kong. Atmos. Chem. Phys. 13(8), 3881-3898.

Guo, H., Ling, Z.H., Simpson, I.J., Blake, D.R., Wang, D.W., 2012b. Observations of isoprene, methacrolein (MAC) and methyl vinyl ketone (MVK) at a mountain site in Hong Kong. J. Geophys. Res.: Atmos. 16;117(D19), doi: 10.1029/2012JD017750.

Guo, H., So, K.L., Simpson, I.J., Barletta, B., Meinardi, S., and Blake, D.R., 2007. C_1-C_8 volatile organic compounds in the atmosphere of Hong Kong: Overview of atmospheric processing and source apportionment. Atmos. Environ. 41(7), 1456-72.

Guo, H., Wang, D.W., Cheung, K., Ling, Z.H., Chan, C.K., and Yao, X.H., 2012a. Observation of aerosol size distribution and new particle formation at a mountain site in subtropical Hong Kong. Atmos. Chem. Phys. 12(20), 9923-9939.

Haddad, I.E., Marchand, N., Temime-Roussel, B., Wortham, H., Piot, C., Besombes, J.L., Baduel, C., Voisin, D., Armengaud, A., and Jaffrezo, J.L., 2011. Insights into the secondary fraction of the organic aerosol in a Mediterranean urban area: Marseille. Atmos. Chem. Phys. 11(5), 2059-2079.

Huang, J.P., Fung, J.C., and Lau, A.K., 2006. Integrated processes analysis and systematic meteorological classification of ozone episodes in Hong Kong. J. Geophys. Res.: Atmos. 111(D20), doi: 10.1029/2005JD007012.

Ho, K.F., Lee, S.C., Guo, H., and Tsai, W.Y., 2004. Seasonal and diurnal variations of volatile organic compounds (VOCs) in the atmosphere of Hong Kong. Sci. Total Environ. 322(1):155-166.

Hu, D., Bian, Q., Li, T.W., Lau, A. K., and Yu, J.Z., 2008. Contributions of isoprene, monoterpenes, β-caryophyllene, and toluene to secondary organic aerosols in Hong Kong during the summer of 2006. J. Geophys. Res.: Atmos. 113(D22), doi: 10.1029/2008JD010437.

Jang, M., Carroll, B., Chandramouli, B., and Kamens, R.M., 2003. Particle growth by acid-catalyzed heterogeneous reactions of organic carbonyls on preexisting aerosols. Environ. Sci. Technol. 37(17), 3828-3837.

Jang, M., Czoschke, N.M., Lee, S., and Kamens, R.M., 2002. Heterogeneous atmospheric aerosol production by acid-catalyzed particle-phase reactions. Science, 298(5594), 814-817.

Janhall, S., Andreae, M.O., and Poschl, U., 2010. Biomass burning aerosol emissions from vegetation fires: particle number and mass emission factors and size distributions. Atmos. chem. Phys. 10(3), 1427-1439.

Kleindienst, T.E., Jaoui, M., Lewandowski, M., Offenberg, J.H., Lewis, C.W., Bhave, P.V., and Edney, E.O., 2007. Estimates of the contributions of biogenic and anthropogenic hydrocarbons to secondary organic aerosol at a southeastern US location. Atmos. Environ. 41(37), 8288-8300.

Kroll, J.H., Ng, N.L., Murphy, S.M., Flagan, R.C., and Seinfeld, J.H., 2006. Secondary organic aerosol formation from isoprene photooxidation. Environ. Sci. Technol. 40(6), 1869-1877.

Lee, S., Kim, H.K., Yan, B., Cobb, C.E., Hennigan, C., Nichols, S., Chamber, M., Edgerton, E.S., Jansen, J.J., Hu, Y., Zheng, M., Weber, R., and Russell, A.G., 2008. Diagnosis of aged prescribed burning plumes impacting an urban area. Environ. Sci. Technol. 42(5), 1438-1444.

Lewandowski, M., Jaoui, M., Offenberg, J.H., Kleindienst, T.E., Edney, E.O., Sheesley, R.J., and Schauer, J.J. (2008). Primary and secondary contributions to ambient PM in the midwestern United States. Environ. Sci. Technol. 42(9), 3303-3309.

Ling, Z.H., Guo, H., Lam, S.H.M., Saunders, S.M., and Wang, T., 2014. Atmospheric photochemical reactivity and ozone production at two sites in Hong Kong: Application of a Master Chemical Mechanism–photochemical box model. J. Geophys. Res.: Atmos. 119(17), 10567-10582.

Maria, S.F., Russell, L.M., Gilles, M.K., and Myneni, S.C., 2004. Organic aerosol growth mechanisms and their climate-forcing implications. Science, 306(5703), 1921-1924.

Offenberg, J.H., Lewandowski, M., Jaoui, M., and Kleindienst, T.E., 2011. Contributions of biogenic and anthropogenic hydrocarbons to secondary organic aerosol during 2006 in Research Triangle Park, NC. Aerosol Air Qual. Res. 11(2), 99-108.

Offenberg, J.H., Lewis, C.W., Lewandowski, M., Jaoui, M., Kleindienst, T.E., and Edney, E.O., 2007. Contributions of toluene and α-pinene to SOA formed in an irradiated toluene/α-pinene/NO x/air mixture: Comparison of results using ^{14}C content and SOA organic tracer methods. Environ. Sci. Technol. 41(11), 3972-3976.

Pope III, C.A., and Dockery, D.W., 2006. Health effects of fine particulate air pollution: lines that connect. J. Air Waste Manage. Assoc. 56(6), 709-742.

562 Reda, A.A., Schnelle-Kreis, J., Orasche, J., Abbaszade, G., Lintelmann, J., Arteaga-Salas, J.M.,
563 Stengel, B., Rade, R., Harndorf, H., Sippula, O., Streibel, T., and Zimmermann, R., 2014. Gas
564 phase carbonyl compounds in ship emissions: Differences between diesel fuel and heavy fuel oil
565 operation. Atmos. Environ. 94, 467-478.
566 Reid, J.S., Koppmann, R., Eck, T.F., and Eleuterio, D.P., 2005. A review of biomass burning
567 emissions part II: intensive physical properties of biomass burning particles. Atmos. Chem. Phys.
568 5(3), 799-825.
569 Rudolph, J., Khedim, A., Koppmann, R., and Bonsang, B., 1995. Field study of the emissions of
570 methyl chloride and other halocarbons from biomass burning in western Africa. J. Atmos. Chem.
571 22(1-2), 67-80.
572 Sippula, O., Stengel, B., Sklorz, M., Streibel, T., Rabe, R., Orasche, J., Lintelmann, J., Michalke,
573 B., Abbaszade, G., Radischat, C., Groger, T., Schnelle-Kreis, J., Harndorf, H., and Zimmermann,
574 R., 2014. Particle emissions from a marine engine: chemical composition and aromatic emission
575 profiles under various operating conditions. Environ. Sci. Technol. 48(19), 11721-11729.
576 So, K.L., and Wang, T., 2003. On the local and regional influence on ground-level ozone
577 concentrations in Hong Kong. Environ. Pollut. 123(2), 307-317.
578 Stocker, T.F., Qin, D., Plattner, G.K., et al. IPCC, 2013: climate change 2013: the physical
579 science basis. Contribution of working group I to the fifth assessment report of the
580 intergovernmental panel on climate change [J]. 2013.
581 Surratt, J.D., Lewandowski, M., Offenberg, J.H., Jaoui, M., Kleindienst, T.E., Edney, E.O., and
582 Seinfeld, J.H., 2007. Effect of acidity on secondary organic aerosol formation from isoprene.
583 Environ. Sci. Technol. 41(15), 5363-5369.
584 Volkamer, R., Jimenez, J.L., San Martini, F., Dzepina, K., Zhang, Q., Salcedo, D., Molina, L.T.,
585 Worsnop, D.R., and Molina, M.J., 2006. Secondary organic aerosol formation from
586 anthropogenic air pollution: Rapid and higher than expected. Geophys. Res. Lett. 33(17), doi:
587 10.1029/2006GL026899.
588 Williams, B.J., Jayne, J.T., Lambe, A.T., Hohaus, T., Kimmel, J.R., Sueper, D., Brooks, W.,
589 Williams, L.R., Trimborn, A.M., Martinez, R.E., Hayes, P.L., Jimenez, J.L., Kreisberg, N.M.,
590 Hering, S.V., Worton, D.R., Goldstein, A.H., and Worsnop, D.R., 2014. The first combined
591 thermal desorption aerosol gas chromatograph-aerosol mass spectrometer (TAG-AMS). Aerosol
592 Sci. Technol. 48(4), 358-370.

Observation of SOA tracers at a mountainous site in Hong Kong: chemical characteristics, origins and implication on particle growth

X.P. Lyu [1], H. Guo [1*], H.R. Cheng [2**], X.M. Wang [3], X. Ding [3], H.X. Lu [1], D.W. Yao [1], and C. Xu [1]

[1] Department of Civil and Environmental Engineering, The Hong Kong Polytechnic University, Hong Kong

[2] Department of Environmental Engineering, School of Resource and Environmental Sciences, Wuhan University, Wuhan, China

[3] State Key Laboratory of Organic Geochemistry, Guangzhou Institute of Geochemistry, Chinese Academy of Sciences, Guangzhou, China

Corresponding author: H. Guo (ceguohai@polyu.edu.hk); H.R. Cheng (chenghr@whu.edu.cn)

Abstract: Secondary organic aerosol (SOA) is an important constituent of airborne fine particles. $PM_{2.5}$ (particles with aerodynamic diameters ≤ 2.5 μm) samples were collected at a mountainous site in Hong Kong in autumn of 2010, and analyzed for SOA tracers. Results indicated that the concentrations of isoprene SOA tracers (54.7±22.7 ng/m^3) and aromatics SOA tracers (2.1±1.6 ng/m^3) were on relatively high levels in Hong Kong. Secondary organic carbon (SOC) derived from isoprene, monoterpenes, sesquiterpenes and aromatics was estimated with the SOA tracer based approach, which constituted 0.35±0.15 μg/m^3 (40.6±5.7%), 0.20±0.03 μg/m^3 (30.4±5.5%), 0.05±0.02 μg/m^3 (5.6±1.7%) and 0.26±0.20 μg/m^3 (21.3±8.2%) of the total estimated SOC. Biogenic SOC (0.60±0.18 μg/m^3) dominated over anthropogenic SOC (0.26±0.20 μg/m^3) at this site. In addition to the total estimated SOC (17.8±4.6% of organic carbon (OC) in $PM_{2.5}$), primary organic carbon (POC) emitted from biomass burning also accounted for a considerable proportion of OC (11.6±3.2%). Insight into the OC origins found that regional transport significantly (p<0.05) elevated SOC from 0.37±0.17 to 1.04±0.39 μg/m^3. Besides, SOC load could also increase significantly if there was influence from local ship emission. Biomass burning related POC in regional air masses (0.81±0.24 μg/m^3) was also higher (p<0.05) than that in samples affected by local air (0.29±0.35 μg/m^3). Evidences indicated that SOA formation was closely related to new particle formation and the growth of nucleation mode particles, while biomass burning was responsible for some particle burst events in Hong Kong. This is the first SOA study in afforested areas of Hong Kong.

Keywords: Secondary organic aerosol, SOA tracer, biogenic SOA, regional transport, particle growth

1. Introduction

Atmospheric aerosol has been well recognized to affect global climate change (Stocker et al, 2013), human health (Dockery et al., 1993; Pope III and Dockery, 2006), visibility (Appel et al., 1985) and sustainability of economy (Chameides et al., 1999). Secondary organic aerosol (SOA) has been identified to play critical roles in these effects (Maria et al., 2004; Volkamer et al., 2006; Baltensperger et al., 2008), thus receiving sufficient attentions in recent years.

So far, the scientific community has reached a consensus that volatile organic compounds (VOCs) from biogenic emissions and anthropogenic aromatics are key precursors of SOA (Forstner et al., 1997; Claeys, et al., 2004). In global scale, biogenic SOA is thought to be the greatest constituent of SOA, due to the worldwide largest emission of biogenic VOCs (*e.g.*, isoprene, monoterpenes and sesquiterpenes) and formation of biogenic SOA spanning a wide range of conditions (the level of NO_x, humidity and aerosol acidity) (Kroll et al., 2006). However, anthropogenic SOA has also been found to be significant in urban areas (Volkamer et al., 2006). Furthermore, upon the findings that biogenic SOA correlates well with the indicators of anthropogenic emissions (Goldstein et al., 2009; Hoyle et al., 2011), it is believed that man-made air pollutants promote the formation of biogenic SOA, in addition to serving as SOA precursors themselves. These promoting effects at least include forming aerosol seeds, catalyzing photooxidation and transformation of biogenic VOCs and their oxidation products and changing the reaction pathways (*e.g.*, atmospheric fate of isoprene in low- and high-NO_x environments) (Hoyle et al., 2011). It is believed that SOA is a collection of hundreds to thousands of organic chemicals featuring relatively low volatilities. To understand SOA formation and explore the potential sources, SOA speciation is of great necessity. However, due to the difficulty in chemical analysis of SOA tracers, the chemical compositions of SOA are far from being well understood. The traditional analysis by gas chromatography-mass spectrometer detector (GC-MSD) generally quantifies a total of less than 20 organic compounds in particles (Offenberg et al., 2007; Kleindienst et al., 2007). Although some advanced instruments have been developed nowadays, such as aerosol mass spectrometry and thermal desorption aerosol gas chromatography, they are either fragment-based or highly dependent upon the skills and knowledge of users (Williams et

al., 2014). Instead, SOA tracer based approach is a simplified method widely used to estimate the amount, precursors and sources of SOA (Kleindienst et al., 2007; Ding et al., 2012).

The SOA tracer based approach applies the laboratory obtained ratios between the sum of specific SOA tracers and total mass of SOA (or secondary organic carbon (SOC)) produced from individual (group of) species to the field measured SOA tracers (Kleindienst et al., 2007), roughly estimating SOA (SOC) derived from an individual VOC or VOC group. Table S1 summarizes the VOC precursors, corresponding SOA tracers and the ratios between SOA tracers and SOA (or SOC), as reported by Kleindienst et al. (2007). The drawbacks of this method are obvious. For instance, it is controversial whether the laboratory obtained ratios can be directly applied to the field measured SOA tracers. However, it provides a feasible approach to estimate the SOA concentration, which is especially helpful in the cases of not well knowing the SOA compositions. More importantly, Offenberg et al. (2007) confirmed that the SOA tracer based approach was reliable through comparing with the results obtained from ^{14}C contents.

Hong Kong, one of the most developed regions in East Asia, has a total territory area of ~1.1×10^3 km^2 and a total population of ~7 million. Despite high population density, it keeps 24 country parks and a vegetation coverage rate of 70%. Evergreen broadleaf trees are common in Hong Kong. Guenther et al. (2006) suggested that shrubs are large emitters of isoprene, a typical and most abundant biogenic VOC. The total emission amount of biogenic VOCs in Hong Kong is estimated as 8.6×10^3 ton C/a (Tsui et al., 2009). Field measurements also revealed that isoprene in Hong Kong is relatively high (300-400 pptv) (Guo et al., 2007, 2012a). In contrast, aromatics are largely emitted from vehicular exhaust and solvent usage in Hong Kong. For example, toluene is one of the most abundant aromatics, with the level of 3-6 ppbv (Guo et al., 2004; Ho et al., 2004). Therefore, local emission of VOCs has a great potential forming SOA in Hong Kong. In addition to local SOA formation, regional transport is inevitable due to severe air pollution in upwind direction of Hong Kong (*i.e.*, inland Pearl River Delta (PRD) region). Studies confirmed that Hong Kong received SOA produced by isoprene and toluene from inland PRD region (Hu et al., 2008). However, the previous SOA studies in Hong Kong all focused on urban areas, which are not enough to understand the abundance, compositions and sources of SOA in low-altitude mountainous area where both anthropogenic and biogenic emissions are important.

In this study, SOC derived from isoprene, monoterpenes, sesquiterpenes and aromatics at a mountainous site in Hong Kong were estimated using a SOA tracer based approach. Local and regional contributions to SOC and biomass burning related POC were determined. Furthermore, in combination with particle size distribution simultaneously monitored by a scanning mobility particle sizer (SMPS), the relationships between SOA formation and particle growth were examined.

2. Methodology

2.1 Sample collection

Hong Kong, a coastal city surrounded by the South China Sea (SCS) to the east and south, is located in southern China. Under the dominance of subtropical monsoon climate, Hong Kong receives northerly winds originating from the heavily polluted PRD region in cool seasons (October-March), while prevailing southerly winds bring in clean air from SCS in warm seasons (April-August) (So and Wang, 2003). The sampling site (22.405° N, 114.118° E, 640 m a.s.l) was set up at the mountainside of the highest mountain in Hong Kong (Mt. Tai Mo Shan with the maximum altitude of 957 m, TMS). The vegetation on this mountain mainly includes Acacia confusa, Lophotemon confertus, Machilus chekiangensis and Schima superba below 550 m, while it turns to shrubs and grasses above 550 m (Guo et al., 2012b). As demonstrated in previous studies (Guo et al., 2013; Ling et al., 2014), regional transport of air pollutants from inland PRD, mesoscale circulation (mountain-valley breezes) and in situ atmospheric chemistry are the main processes that significantly influence air quality at this site. Figure 1 shows the geographical locations of the sampling site and air quality monitoring stations (AQMSs) of Hong Kong Environmental Protection Department (HKEPD).

From September 7 to November 26, 2010, a total of 19 $PM_{2.5}$ samples were collected. The instrument was an Anderson high volume $PM_{2.5}$ sampler, with a flow rate of 750 L/min. Pre-baked A4 size quartz fiber filters were used to collect the samples, which were stored in the refrigerator at -18 °C after sampling. Generally, each filter sampling lasted for 45-55 hours, except for the cases that the instrument stopped abnormally on some days due to thunderstorm-caused power outages. Table S2 lists the sample IDs, start and end dates & times. The origins of air masses, as distinguished by wind field and ratio of SO_2/NO_x (see section 3.3 for details), are also shown in the table. Additionally, the particle number concentrations and size distributions in the size range of 5.5-350.4 nm in 44 size bins were monitored by a scanning mobility particle

sizer (SMPS) from October 27 to November 29. Detailed introductions about the operation procedures of SMPS and data processing can be found in Guo et al. (2012a). We also collected ambient VOC samples during September 28-November 21. Inorganic trace gases (SO_2, CO, NO, NO_2 and O_3) and weather conditions were measured simultaneously with the $PM_{2.5}$ sampling. Details about VOC sampling, VOC analysis and monitoring of trace gases are provided in Guo et al. (2013) and Ling et al. (2014).

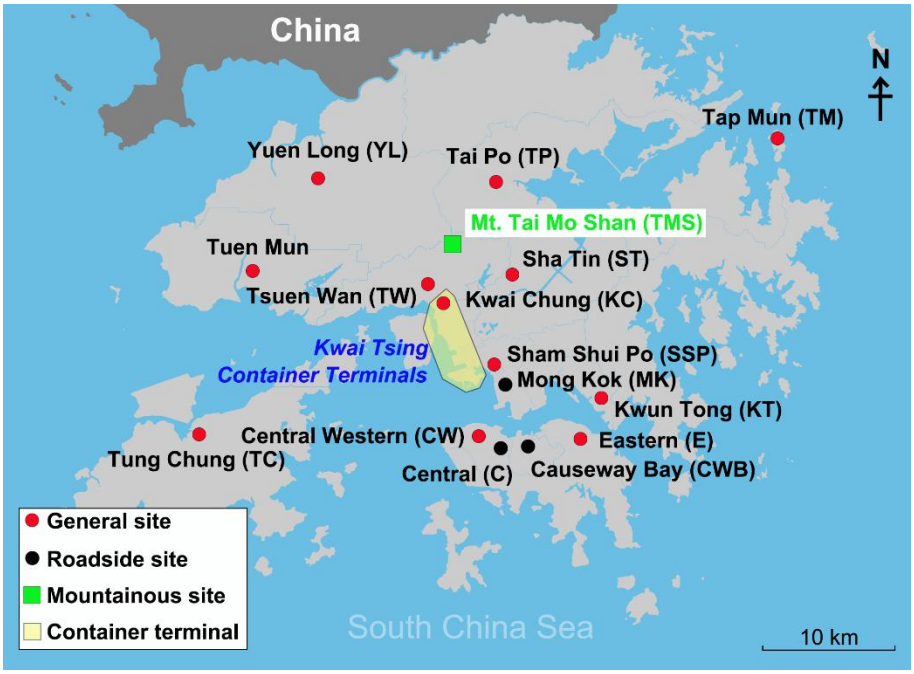

Figure 1 Geographic locations of the sampling site (TMS), AQMSs of HKEPD and the container terminal area where nine container terminals are located. Capital letters in the brackets are abbreviations of the site/stations

2.2 Chemical analysis

OC and element carbon (EC) in $PM_{2.5}$ samples were analyzed using the thermo-optical transmittance method recommended by National Institute for Occupational Safety and Health (NIOSH) (Birch, 1998). The concentrations of OC and EC are shown in Figure S1.

The method of SOA analysis was in line with that introduced by Ding et al. (2011). Briefly, the procedures for each sample include solvent extraction, derivation, analysis by GC-MSD, and identification and quantification of SOA tracers. 1/8 of each filter was extracted three times by sonication in the solvent of 40 mL of 1:1 (v/v) dichloride methane (DCM)/methanol mixture. Prior to extraction, the internal standards (hexadecanoic acid-D_{31}, phthalic acid-D_4 and

levoglucosan-$^{13}C_6$) were spiked into the samples. The three-time extracts of each sample were combined, filtered and concentrated to ~2 mL, which was further divided into two parts for methylation and silylation derivation, respectively. In methylation derivation, the extract experienced a gentle nitrogen blow to dryness, and subsequent addition of 200 μL of DCM, 10 μL of methanol and 300 μL of freshly prepared diazomethane. Then, it was kept in room temperature for one hour to derivatize acids to methyl esters, after which the sample was blown to 200 μL and used for analysis of some *α*-pinene SOA tracers (Pinonic acid, pinic acid and 3-methyl-1,2,3-butanetricarboxylic acid). The silylation reagent was 100 μL of pyridine and 200 μL of N,O-bis-(trimethylsilyl)-trifluoroacetamide (BSTFA) plus 1% trimethylchlorosilane (TMCS). Differently, the derivation was carried out in an oven at 70 °C for one hour. One *α*-pinene SOA tracer (3-hydroxyglutanic acid) and tracers for isoprene SOA, sesquiterpenes SOA, and toluene SOA were analyzed from the silylated sample. An Agilent 5973N GC/MSD was employed to do the analysis. The identification of SOA tracers was based on the comparison of mass spectra with previous studies, and their retention time in GC chromatogram with other known compounds as the references. Pinonic acid and pinic acid were quantified by authentic standards. However, due to lack of standards, other *α*-pinene SOA tracers, isoprene SOA tracers, *β*-Caryophyllenic acid and 2,3-dihydroxy-4-oxopentanoic acid were quantified using pinic acid (PA), erythritol, octadecanoic acid and azelaic acid, respectively. The detection limits (DLs) for pinonic acid, pinic acid, erythritol, octadecanoic acid and azelaic acid were 0.05, 0.07, 0.06, 0.09, and 0.11 ng/m^3, respectively. Levoglucosan was also quantified with the DL of 0.15 ng/m^3. The SOA tracers analyzed in this study are highlighted in Table S1.

2.3 Quality assurance and quality control

In this study, internal standards were not spiked on the filters before sampling, to avoid their influences on OC analysis. According to the saturation concentrations of SOA tracers calculated by Ding et al. (2016), SOA tracers analyzed in this study were of low volatilities, except for pinonic acid. Therefore, pinonic acid in airborne $PM_{2.5}$ might be underestimated due to the blow-off effect during sampling, which however should not be significant to other SOA tracers. Recovery target compounds were spiked in the samples before analysis of SOA tracers. The recovery rates were 104±2%, 68±13%, 62±14%, 78±10%, 81±9% and 87±4% for pinonic acid, pinic acid, erythritol, octadecanoic acid, azelaic acid and levoglucosan, respectively. Since

internal standards were added into the samples prior to analysis, we did not use the recovery rates to correct the concentrations of SOA tracers.

2.4 Processing of SMPS data

In this study, particles measured by SMPS were divided into nucleation (5.5-24.7 nm), Aitken (24.7-101.4 nm) and accumulation modes (101.4-350.4 nm). Geometric mean diameter (GMD) for nucleation mode particles (5.5-24.7 nm) was calculated using the following equations (Guo et al., 2012a).

$$\mathrm{GRs} = \frac{d_{GMD}}{d_t} \quad \text{(Equation (1))}$$

$$\mathrm{GMD} = e^{(\sum n_i ln^{d_i})/N} \quad \text{(Equation (2))}$$

$$\frac{d_N}{d_{log_{D_p}}} = \frac{\Delta N}{log_{D_p^2} - log_{D_p^1}} \quad \text{(Equation (3))}$$

where n_i is the particle number concentration in the i^{th} bin with upper diameter of d_i, N represents the total number concentration (cm^{-3}). ΔN is the particle number concentration in the size bin with upper and lower limit diameter of D_p^2 and D_p^1, respectively.

Condensation sink (CS), which describes the loss rate of vapor molecules and newly formed particles on the pre-existing aerosol particles, was calculated as follows (Kulmala et al., 2005):

$$\mathrm{CS} = 2\pi \mathrm{D} \int D_p \beta_m(D_p) n(D_p) dD_p = 2\pi \mathrm{D} \sum_i \beta_{mi} D_{pi} N_i \quad \text{(Equation (4))}$$

where D is the diffusion coefficient of the condensing vapor, β_m is the transitional regime correction factor, D_p denotes the particle diameter, n and N represent the particle numbers. β_{mi}, D_{pi} and N_i are the specific values for a given size bin (i). Growth factor calculated according to Laakso et al. (2004) was used to calibrate the dry particle size measured by SMPS.

3. Results and discussion

3.1 Concentrations of SOA tracers

Table 1 shows the average concentrations of SOA tracers derived from different precursors at TMS. Isoprene SOA tracers were the most abundant (54.7±22.7 ng/m^3), followed by the tracers generated from monoterpenes (26.3±4.5 ng/m^3), aromatics (2.1±1.6 ng/m^3) and sesquiterpenes (1.1±0.4 ng/m^3). Figure 2 compares the concentrations of SOA tracers between previous studies and the present study. The number and species of SOA tracers for the same precursor were the same. For the cases that total concentration of monoterpenes SOA tracers was given (*e.g.*, Offenberg et al., 2011), a factor was applied to the total concentration to roughly estimate the

sum of monoterpenes SOA tracers with the number and species identical to this study (see section S1 and Figure S2 in the Supplement). It was found that isoprene SOA tracers at TMS were on relatively high level (54.7±22.7 ng/m^3), comparable to or even higher than those detected in the forest (61.4±30.4 ng/m^3 in Kleindienst et al. (2007) and 39.0±17.2 ng/m^3 in Offenberg et al. (2011)). In fact, isoprene at TMS was relatively low (2-517 pptv), the high isoprene SOA tracers indicated that biogenic SOA formation at this site might be enhanced by anthropogenic emissions, *e.g.*, sufficient aerosol seeds from SO_2-related new particle formation (Guo et al., 2012a). Certainly, regional transport could also contribute to high isoprene SOA tracers, as reported by Hu et al. (2008). For the anthropogenic SOA, the tracer produced by aromatics (2,3-dihydroxy-4-oxopentanoic acid) was noticeable. Although the average 2,3-dihydroxy-4-oxopentanoic acid in this study (2.1±1.6 ng/m^3) was not significantly higher than that in other studies (p>0.05), its maximum value reached 13.5 ng/m^3. Given abundant aromatics in the atmosphere of Hong Kong and mesoscale circulations between TMS and the surrounding urban areas, local formation could be an important factor contributing to high aromatics SOA at TMS. Moreover, it was reported that 2,3-dihydroxy-4-oxopentanoic acid at an urban background site in inland PRD was very high (13.1 ng/m^3) (Ding et al., 2012). Hence, regional transport might be partially responsible for the relatively high aromatics SOA tracer in Hong Kong. SOA tracers derived from monoterpenes and sesquiterpenes were on moderate levels, compared to other studies.

3-Methyl-1,2,3-butanetricarboxylic acid and 3-hydroxyglutanic acid, formed from monoterpenes oxidation in the presence of NO_x (Claeys et al., 2007; Eddingsaas et al., 2012), dominated the measured monoterpenes SOA tracers, consistent with those at an urban background site in inland PRD (Ding et al., 2012). Pinonic acid and pinic acid, formed from OH oxidation of α-pinene in NO_x free environment or ozonolysis of α-pinene (Eddingsaas et al., 2012), were also higher than those in urban areas of Hong Kong (almost below DLs) (Hu et al., 2008). Since NO_x was at the magnitude of several ppbv, the higher pinonic acid and pinic acid were likely due to the higher O_3 (69.2±2.4 ppbv at TMS and 30.8±2.6 ppbv at the mountain foot) at this mountainous site. In addition, other tracers including 3-hydroxy-4,4-dimethylglutaric acid, 3-isopropylpentanedioic acid, 3-acetylpentanedioic acid and 3-acetylhexanedioic acid, which were not measured in this study, accounted for 46.9±4.0% of the total amount of tracers according to Kleindienst et al. (2007). Of the isoprene SOA tracers, 2-methylthreitol and 2-methylerythritol are representative

products formed through the photooxidation of isoprene hydroxyhydroperoxides and acid catalysis of epoxydiols of isoprene in low NO_x environment when RO_2 reacting with HO_2 dominated the loss of RO_2 (Claeys et al., 2004; Surratt et al., 2010). In this study, they accounted for 83.5±8.1% of the total isoprene tracers. However, NO_x was not low enough and RO_2 reacting with NO was the main sink of RO_2 (Ling et al., 2014), implying that other mechanisms might enhance the formation of 2-methyltetrols (sum of 2-methylthreitol and 2-methylerythritol) at this site, such as acid catalysis (Surratt et al., 2007).

Table 1 Average concentrations of SOA tracers derived from monoterpenes, isoprene, sesquiterpenes and aromatics (mean±95% confidence interval (C.I.)).

VOC precursor	SOA tracer	Concentration (ng/m^3)
Monoterpenes	Pinonic acid	1.2±0.4
	Pinic acid	2.0±0.6
	3-methyl-1,2,3-butanetricarboxylic acid	16.0±3.5
	3-hydroxyglutanic acid	7.1±2.7
	Sum 1	26.3±4.5
Isoprene	2-Methylthreitol	14.7±6.6
	2-Methylerythritol	31.2±13.1
	2-methylglyceric acid	5.2±3.1
	cis-2-Methyl-1,3,4-trihydroxy-1-butene	0.8±0.5
	trans-2-Methyl-1,3,4-trihydroxy-1-butene	2.0±1.3
	3-Methyl-2,3,4-trihydroxy-1-butene	0.7±0.3
	Sum 2	54.7±22.7
Sesquiterpenes	*β*-Caryophyllenic acid	1.1±0.4
Aromatics	2,3-Dihydroxy-4-oxopentanoic acid	2.1±1.6

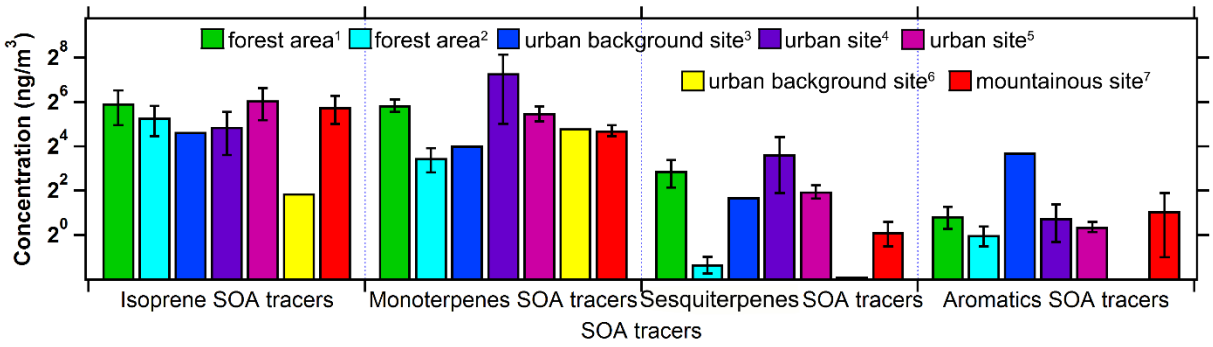

Figure 2 Comparison of SOA tracers between previous studies and this study. [1]Kleindienst et al. (2007); [2]Offenberg et al. (2011); [3]Ding et al. (2012); [4]Hu et al. (2008); [5]Lewandowski et al. (2008); [6]Haddad et al. (2011); [7]this study.

3.2 Estimate of SOC

Both the EC tracer method and SOA tracer method were used to estimate SOC (details about both methods are provided in section S2 of the Supplement). To apply the SOA tracer method, the sum of monoterpenes SOA tracers was scaled by a factor of 1.79 (see section S1 and Figure S2 for details). Figure S3 compares the SOC estimated by these two methods. SOC estimated by EC tracer method ($SOC_{EC\ tracer}$) were generally higher (p<0.01) than those estimated by SOA tracer method ($SOC_{SOA\ tracer}$), except for samples TMS1, TMS3 and TMS8. Ding et al. (2012) indicated that the EC tracer method might overestimate SOC, because it blended some primary OC (POC) from biomass burning with SOC. This inference was supported by the good correlation between the difference of SOC estimated by these two methods ($SOC_{EC\ tracer}$-$SOC_{SOA\ tracer}$) and levoglucosan, a tracer of biomass burning.

In addition to levoglucosan, methyl chloride (CH_3Cl) is an indicator of biomass burning (Rudolph et al., 1995). Figure 3 plots the correlation between levoglucosan and CH_3Cl at TMS, as well as that between $SOC_{EC\ tracer}$-$SOC_{SOA\ tracer}$ and levoglucosan. As expected, levoglucosan fairly correlated with CH_3Cl (R^2=0.54), further confirming the reliability of levoglucosan as the tracer of biomass burning. Consistent with Ding et al. (2012), good correlation was found between $SOC_{EC\ tracer}$-$SOC_{SOA\ tracer}$ and levoglucosan (R^2=0.52). This verified that the EC tracer method overestimated SOC due to the interference of biomass burning. Exceptionally, $SOC_{EC\ tracer}$ was remarkably lower than $SOC_{SOA\ tracer}$ for the samples TMS1, TMS3 and TMS8 (p<0.05). Further investigation found that on the sampling days of TMS1 and TMS3, the daily maximum hourly O_3 mixing ratio, referred to as peak O_3, was extremely high, with the values being the

second (154.4 ppbv) and first (163.4 ppbv) highest among the 19 filter samples, respectively, while during the sampling period of TMS8, the peak O_3 also reached 94.8 ppbv. In contrast, the average of peak O_3 values on the sampling days of other $PM_{2.5}$ filter samples was only 77.6 ppbv. Since high O_3 levels generally imply strong photochemical reactivity, high productions of SOA are also expected on these days. Hence, the higher $SOC_{SOA\ tracer}$ values observed in TMS1, TMS3 and TMS8 were understandable. We also found that there was no correlation between $SOC_{EC\ tracer}$ and peak O_3 (not shown), whereas $SOC_{SOA\ tracer}$ correlated well with peak O_3 (R^2=0.68), as shown in Figure 4, implying that the formation of secondary products, *i.e.*, SOA and O_3, depends upon the oxidative capacity of the atmosphere and they may also influence each other. Therefore, the SOA tracer method was believed to be more reliable and thus adopted in this study. Hereafter, SOC refers to $SOC_{SOA\ tracer}$, unless otherwise specified.

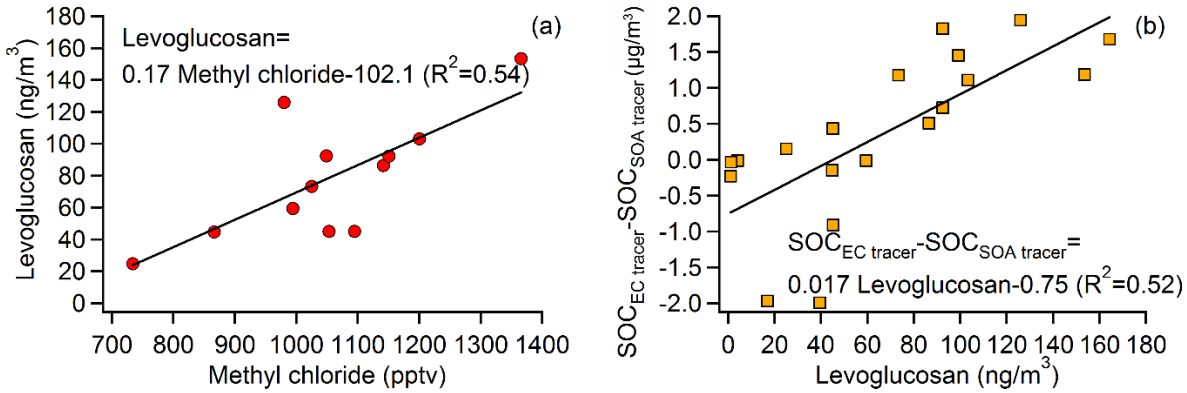

Figure 3 Linear correlations between (a) levoglucosan and CH_3Cl, and (b) $SOC_{EC\ tracer}$-$SOC_{SOA\ tracer}$ and levoglucosan.

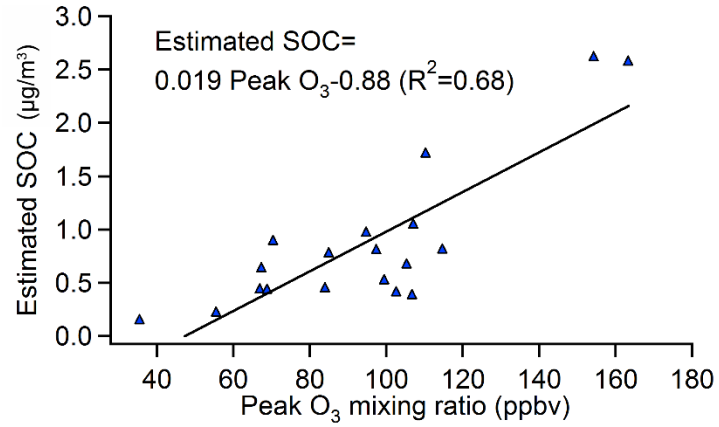

Figure 4 Linear correlation between $SOC_{SOA\ tracer}$ and peak O_3.

Figure 5 shows SOC produced by different groups of VOCs estimated using the SOA tracer based approach, and biomass burning related POC ($POC_{biomass\ burning}$). $POC_{biomass\ burning}$ was estimated by 0.01 (μg/ng) × levoglucosan (ng/m^3) (Lee et al., 2008). On average, SOC and $POC_{biomass\ burning}$ constituted 0.86±0.31 μg/m^3 (17.8±4.6%) and 0.67±0.22 μg/m^3 (11.6±3.2%) of OC (provided in Figure S1), respectively. The rest of OC were undetermined due to unknown sources and precursors of OC. The total SOC comprised anthropogenic (*i.e.*, aromatics) and biogenic (*i.e.*, isoprene, monoterpenes and sesquiterpenes) SOC, with the fractions of 21.3±8.2% (0.26±0.20 μg/m^3) and 78.7±8.2% (0.60±0.18 μg/m^3), respectively. Although anthropogenic SOC (ASOC) was significantly lower than biogenic SOC (BSOC) (p<0.05), ASOC had its highest value of 1.71 μg/m^3 in the sample TMS1, and BSOC reached its maximum in sample TMS3 (2.03 μg/m^3). As mentioned earlier, the two samples were collected on the days with very high O_3, indicating that aromatics and biogenic VOCs might be responsible for the high SOC in TMS1 and TMS3, respectively. However, VOC samples were not simultaneously collected during the collection of these two samples. Instead, the sample TMS12 was a good example because ASOC was the second highest (1.2 μg/m^3), and the daily average mixing ratio of toluene coincidently reached 4.0 ppbv during the TMS12 sampling period, the highest value among all VOC samples, which further confirmed the reliability of SOA tracer method in estimating SOC. Among SOC derived from biogenic VOCs, isoprene made the highest contribution (54.2±5.3% of BSOC and 42.7±5.9% of total SOC), followed by monoterpenes (37.9±4.6% and 30.4±5.5%, respectively) and sesquiterpenes (7.9±2.7% and 5.6±1.7%, respectively).

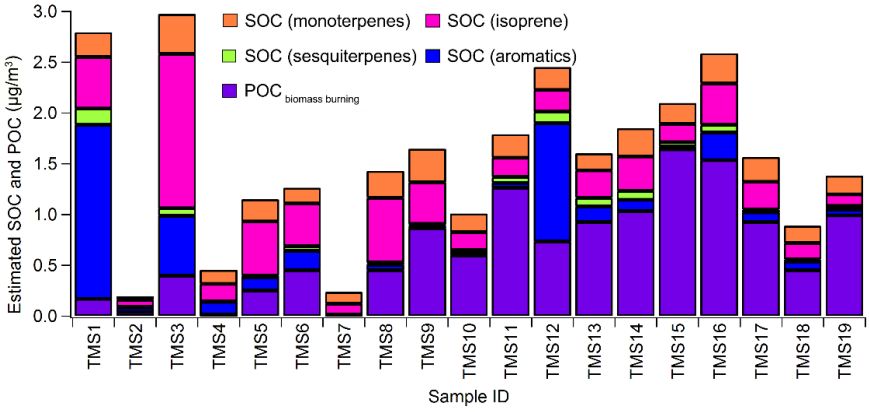

Figure 5 Concentrations of estimated SOC derived from monoterpenes, isoprene, sesquiterpenes and aromatics and $POC_{biomass\ burning}$.

3.3 Local and regional contributions to SOC

In line with the method used in Guo et al. (2013), the local and regional air masses were distinguished with the wind direction (WD) and wind speed (WS) monitored at TMS. Briefly, the northerly winds (0°<WD<90° or 270°<WD<360°) with WS higher than 2 m/s were considered to be capable of delivering air pollutants from the heavily polluted inland PRD region to the site. In these cases, the air masses were believed to be subject to regional influences. Otherwise, the site was dominated by local air. To validate this method, Figure 6 shows the hourly ratios of SO_2/NO_x for the air masses in different wind directions/speeds. Overall, the SO_2/NO_x ratios were higher for regional air masses, particularly when 0°<WD<90° and WS>2 m/s. This coincided with the lower sulfur content in vehicle fuels and higher vehicle emissions of NO_x in Hong Kong (Wang and So, 2003; Guo et al., 2009). For the 24-48 hr $PM_{2.5}$ samples (*i.e.*, duration of 1-2 days), the regional influence was not unexpected given that the northerly wind was stronger than 2 m/s for at least one hour on each sampling day. It was noteworthy that during the sampling periods of TMS1 and TMS16 (influenced by regional air), SO_2 was exclusively high at the HKEPD AQMSs in vicinity of the ship container terminals, *e.g.*, KC, SSP and TW (see Figure 1). Figure S4 presents SO_2 distributions at 14 AQMSs in Hong Kong during these two periods. In view of the fact that ship is a significant emitter of SO_2, the influence of local ship emission was also suspected for the two samples. According to these inferences, Table S2 lists the categories of the samples affected by regional air, local air, and local ship emissions, respectively.

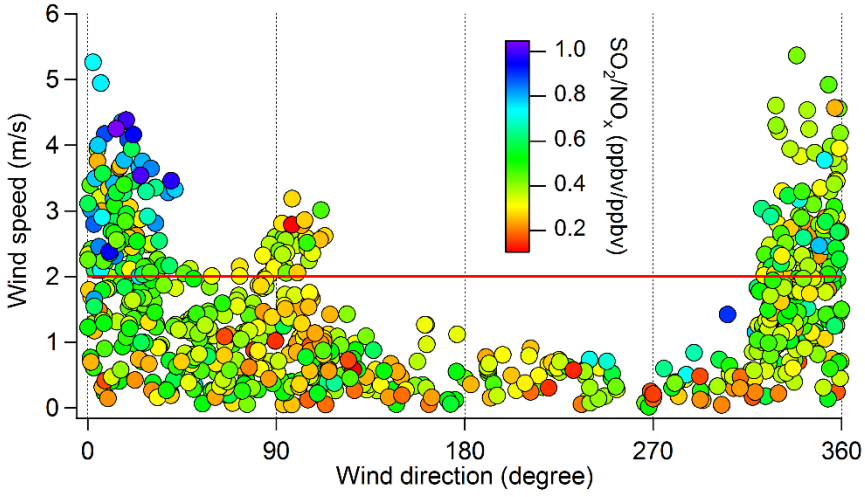

Figure 6 Hourly ratios of SO_2/NO_x for the air masses in different wind directions/speeds at TMS.

Table 2 summarizes the concentrations of SOC and $POC_{\text{biomass burning}}$ in different categories of air masses. Note that since the samples TMS1 and TMS16 were influenced by both regional air and local ship emission, they were separately discussed later. It was found that SOC derived from

individual group/species and total SOC in regional air were all significantly (p<0.05) higher than that in local air, suggesting that SOC at TMS was elevated by regional transport. Despite possible influences of local ship emissions in TMS1 and TMS16, the concentrations of SOC and POC in these two samples were well within the ranges of those in regional air, except for aromatics SOC (1.71 μg/m^3) in sample TMS1. The extremely high aromatics SOC in TMS1 might be caused by ship emissions which could be laden with high concentrations of aromatics. Contradictorily, SOC derived from aromatics was remarkably lower in TMS16 (0.27 μg/m^3). This discrepancy might be explained by the differences of fuel types and operating conditions of the ship engines, which were repeatedly proved to affect the emission characteristics of ship engines (Reda et al., 2014; Sippula et al., 2014). Similar to SOC, POC also showed a significantly higher level in regional air (0.81±0.24 μg/m^3) than that in local air (0.29±0.35 μg/m^3) (p<0.05). Since the high concentration of $POC_{biomass\ burning}$ in regional air was partially contributed by TMS16 ($POC_{biomass\ burning}$ =1.54 μg/m^3), a sample jointly influenced by regional air and local ship emission, specific insight was given to this sample. Firstly, ship emission was not likely to be the culprit of high $POC_{biomass\ burning}$, as no study reported ship emission of levoglucosan, the biomass burning tracer used to calculate $POC_{biomass\ burning}$ in this study. Instead, we found that another sample under the influence of regional air (TMS15) had comparable $POC_{biomass\ burning}$ (1.64 μg/m^3). Furthermore, CH_3Cl, another tracer of biomass burning, increased noticeably under northerly winds in sample TMS16, indicating the regional transport of biomass burning plumes into Hong Kong. In fact, nearly no fire spot in local Hong Kong was observed by the satellite during the sampling, compared to some open fires detected in upwind directions (see Figure S5). Therefore, $POC_{biomass\ burning}$ in TMS16 was reasonably speculated to be elevated by regional biomass burning plumes. Upon this inference, we concluded that regional transport significantly contributed to $PM_{2.5}$-bounded POC in Hong Kong.

Table 2 Mean±95% C.I. of SOC and POC in different categories of air masses (Unit: μg/m^3).

	Local air	Regional air	TMS1*	TMS16*
SOC (monoterpenes)	0.13±0.06	0.23±0.03	0.23	0.28
SOC (isoprene)	0.16±0.07	0.42±0.18	0.51	0.41
SOC (sesquiterpenes)	0.01±0.01	0.06±0.02	0.16	0.07
SOC (aromatics)	0.07±0.04	0.33±0.26	1.71	0.27

$POC_{biomass\ burning}$	0.29±0.35	0.81±0.24	0.17	1.54
Total SOC	0.37±0.17	1.04±0.39	2.61	1.04

[*] 95% C.I. is not available for a single sample.

3.4 Implications to particle formation and growth

As an important constituent of airborne particles, SOA plays critical role in particle formation and growth (Jang et al., 2003). The relationships between SOA formation and particle formation/growth were investigated on three selected days (October 31, November 09 and November 19) when SOC were among the highest of all the samples and SMPS data were available. Figures 7-9 show the evolutions of particle numbers, GMD of nucleation mode particles, CS, the simulated sulfuric acid (SA) vapor, oxidized intermediates of aromatics (AOI), oxidized intermediates of biogenic VOCs (BOI), and the measured inorganic trace gases. Details about the modelling of SA vapor, AOI and BOI are provided in Section S3 and Table S3 in the Supplement. For convenience of analysis, the hourly mixing ratios of biogenic VOCs (BVOCs), aromatics and CH_3Cl are presented in Figure S6.

In Figures 7-8, the number concentration of nucleation mode particles (N_{nuc}) increased substantially in the morning of October 31 (11:00-12:00) and November 09 (10:00-11:00), followed by the increases of number of Aitken mode particles (N_{Ait}). Prior to the increases of N_{nuc}, the simulated SA vapor began to increase about 3 hours earlier. These were consistent with the findings in Guo et al. (2012a) who reported that the increase of N_{nuc} was caused by new particle formation (NPF) events occurred on both days, and SA vapor played important roles in NPF. However, we further found that the oxidation intermediates of BVOCs (*i.e.*, BOI) also increased slightly ahead of the rise of N_{nuc}, which might suggest that the oxidation of BVOCs also made some contributions to NPF. In fact, the involvement of BVOCs in NPF at this afforested site has been speculated by Guo et al. (2012a), which is confirmed with the aid of model simulations in this study.

Moreover, we noticed that the nucleation mode particles experienced obvious growth with the rate of 1.9 nm/h (15:00-16:00) and 1.4 nm/h (14:00-16:00) in the afternoon of October 31 and November 09, respectively. Both growths occurred under the conditions of high N_{Ait} and high CS, differing from NPF events. Meanwhile, O_3 was on high level, which meant strong oxidative capacity of the atmosphere. Correspondingly, the simulated SA vapor, AOI and BOI showed great increments simultaneously with or 1-2 hours earlier than the increase of GMD. It is

noteworthy that the significant increases of AOI and BOI were also attributable to the rapid increases of VOCs (see Figure S6), in addition to strong atmospheric oxidative capacity. This suggested that the photo-oxidation of VOCs also facilitated the growth of nucleation mode particles. The prompt responses of particle growth to the increments of oxidation products on October 31 (rather than 1.5 hours' delay on November 09) were likely caused by the much more abundant BOI (~22.7 pptv) than that on November 09 (~13.5 pptv). Besides, the lower initial GMD before its increase on October 31 (~14 nm compared to ~16 nm on November 09) implied higher surface area and subsequently quicker growth. Since the aforementioned days featured high SOA, the roles of photo-oxidation of VOCs in the formation and growth of nucleation mode particles might reflect the very initial stages of SOA formation. However, to better understand the relationships between SOA formation and the formation/growth of particles, data with higher resolution and more comprehensive chemical information of SOA are crucially needed.

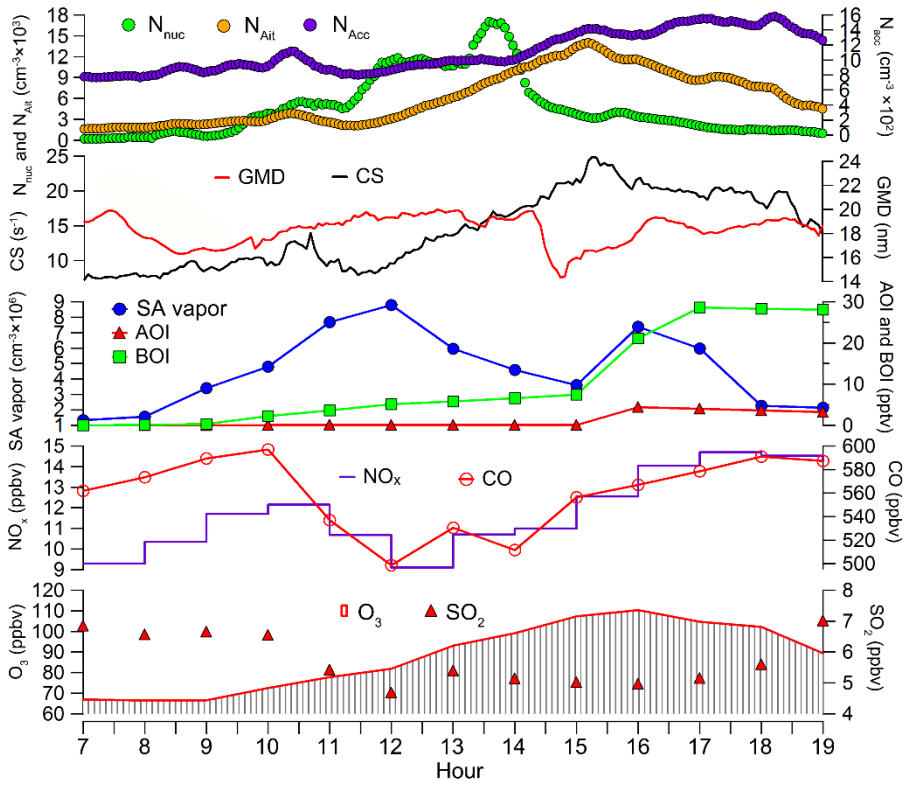

Figure 7 Evolutions of particle numbers, GMD of nucleation mode particles, CS, simulated SA vapor, AOI, BOI and inorganic trace gases on October 31 (first sampling day of TMS12).

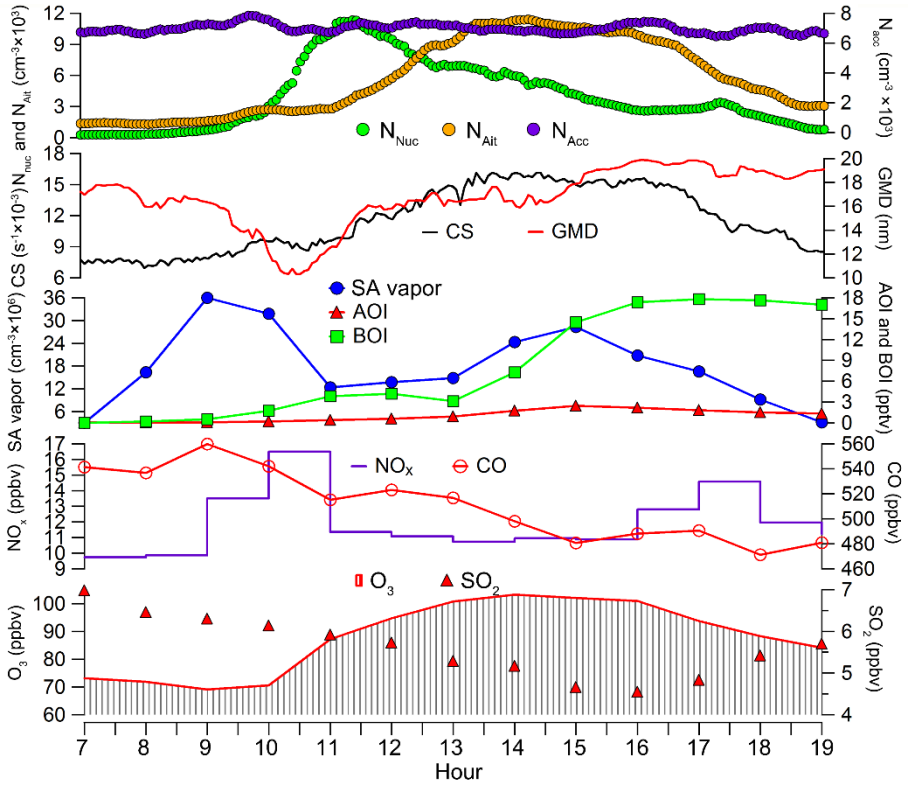

Figure 8 Evolutions of particle numbers, GMD of nucleation mode particles, CS, simulated SA vapor, AOI, BOI and inorganic trace gases on November 09 (second sampling day of TMS14).

Similarly, the growth of nucleation mode particles was also observed on November 19 (15:00-16:00) (Figure 9). However, a distinct phenomenon was that the numbers of particles in nucleation, Aitken and accumulation modes all showed rapid increases simultaneously from around 14:30 and reached the highest values at ~15:00, which indicated that the particles in different modes shared a common source. Although SO_2 and the simulated SA vapor began to increase 1.5 hours earlier, this could not be a NPF event, as the increase of N_{Ait} had no delay (no banana shape) and the CS was high. In addition, the levels of primary air pollutants (*e.g.*, NO_x and CO) were high at the peak hours of all three-mode particle numbers. More importantly, we found that CH_3Cl largely increased from 13:00 to 15:00 and reached the maximum at 15:00 (see Figure S6). Therefore, we suspected that biomass burning might be responsible for the increase of particle numbers. This coincided with the high $POC_{\text{biomass burning}}$ (1.54 μg/m^3) in $PM_{2.5}$ sample collected on this day (TMS16). Generally, particles emitted from biomass burning are in Aitken and accumulation modes (Reid et al., 2005). However, in vicinity of fire, nucleation mode can also exist (Janhall et al., 2010). Here, although nucleation mode particles increased in the particle

burst event, N_{nuc} was very low (maximum=2.1×10^3 cm^{-3}), indicating that this was not a local biomass burning and nucleation mode particles converted to larger size particles from the source region to this site. This was also consistent with the regional influence on this day identified by the wind fields (see section 3.3).

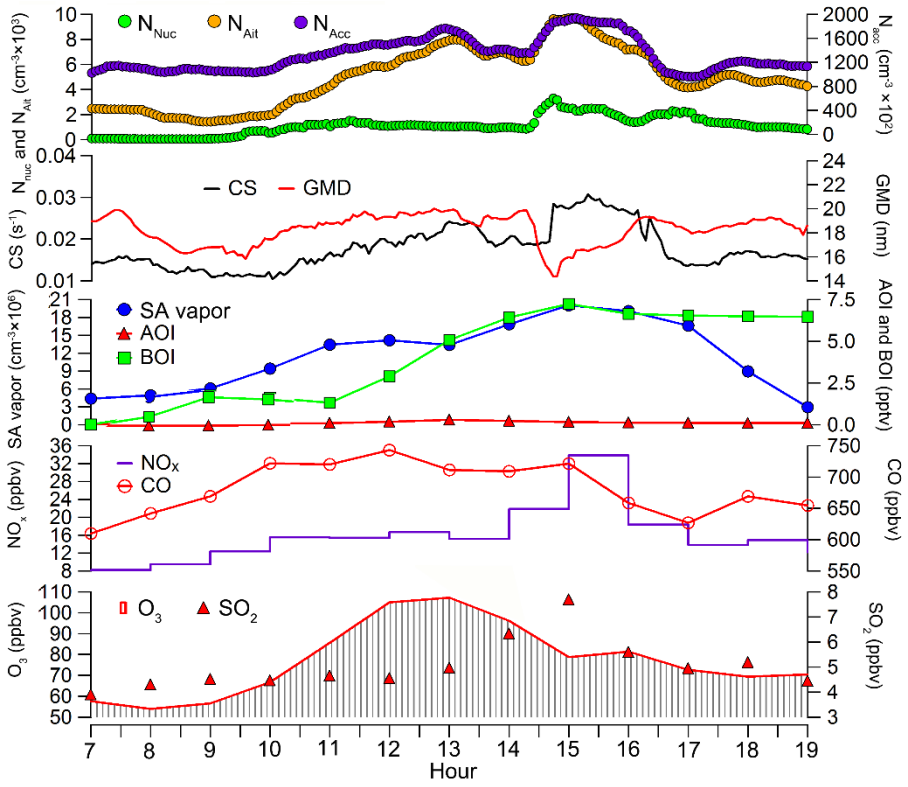

Figure 9 Evolutions of particle numbers, GMD of nucleation mode particles, CS, simulated SA vapor, AOI, BOI and inorganic trace gases on November 19 (sampling day of TMS16).

4. Conclusions

$PM_{2.5}$ samples were collected at a mountainous site in Hong Kong in autumn of 2010. Nine SOA tracers in $PM_{2.5}$ were analyzed, which helped to understand the compositions and sources of SOC in this study. Results indicated that isoprene made the highest contribution to SOC formation at this site, followed by monoterpenes, aromatics and sesquiterpenes. Averagely, biogenic SOC dominated over anthropogenic SOC. However, anthropogenic SOC cannot be neglected, particularly under the influences of regional transport (*e.g.*, 1.2 μg/m^3 in sample TMS12) and/or local ship emission (*e.g.*, 1.7 μg/m^3 in sample TMS1). The simultaneous observation of VOCs confirmed the role of aromatics in contributing to high concentrations of anthropogenic SOC. In terms of SOC origins, regional transport caused nearly two-fold increase

of SOC, relative to local air. However, SOC load could also be significantly elevated by local ship emissions possibly containing abundant VOC precursors and SO_2, which promoted SOC formation. In addition, the regional air was generally characterized with high biomass burning related POC, aggravating the $PM_{2.5}$-bounded POC in Hong Kong. In combination with the SMPS data, we found that the formation of SOA (particularly the biogenic SOA) might be partially responsible for the new particle formation and growth of nucleation mode particles. Primary emissions, such as biomass burning, could cause particle burst events and lead to POC increases. To our knowledge, this is the first SOA study carried out in low-altitude (640 m) mountainous area of Hong Kong, where the air quality is under the combined influence of anthropogenic and biogenic emissions. This study also demonstrates the urgency of data acquisition with more comprehensive chemical information and higher time resolution in future SOA studies over this region.

Acknowledgements

This study was supported by the Research Grants Council of the Hong Kong Special Administrative Region via grants CRF/C5004-15E, PolyU5154/13E, PolyU152052/14E, and CRF/C5022-14G, and the Hong Kong Polytechnic University PhD scholarships (project #RTUP). This study is partly supported by the Hong Kong PolyU internal grant (1-BBW4, 4-ZZFW, G-YBHT and 1-ZVJT) and by the Innovation and Technology Commission of the HKSAR via the Hong Kong Branch of National Rail Transit Electrification and Automation Engineering Technology Research Center (1-BBYD).

References

Appel, B.R., Tokiwa, Y., Hsu, J., Kothny, E.L., and Hahn, E., 1985. Visibility as related to atmospheric aerosol constituents. Atmos. Environ. (1967), 19(9), 1525-1534.

Birch, M.E., 1998. Analysis of carbonaceous aerosols: interlaboratory comparison. Analyst 123(5), 851-857.

Chameides, W.L., Yu, H., Liu, S.C., Bergin, M., Zhou, X., Mearns, L., Wang, G., Kiang, C.S., Saylor, R.D., Luo, C., Huang, Y., Steiner, A., and Giorgi, F., 1999. Case study of the effects of atmospheric aerosols and regional haze on agriculture: An opportunity to enhance crop yields in China through emission controls?. P. Natl. Acad. Sci. 96(24), 13626-13633.

Claeys, M., Graham, B., Vas, G., Wang, W., Vermeylen, R., Pashynska, V., Cafmeyer, J., Guyon, P., Andreae, M., Artaxo, P., and Maenhaut, W., 2004. Formation of secondary organic aerosols through photooxidation of isoprene. Science 303(5661), 1173-1176.

Claeys, M., Szmigielski, R., Kourtchev, I., Van der Veken, P., Vermeylen, R., Maenhaut, W., Jaoui, M., Kleindienst, T.E., Lewandowski, M., Offenberg, J.H. and Edney, E.O., 2007. Hydroxydicarboxylic acids: markers for secondary organic aerosol from the photooxidation of α-pinene. Environ. Sci. Technol. 41(5), 1628-1634.

Ding, X., Wang, X.M., Gao, B., Fu, X.X., He, Q.F., Zhao, X.Y., Yu, J.Z., and Zheng, M., 2012. Tracer-based estimation of secondary organic carbon in the Pearl River Delta, south China. J. Geophys. Res.: Atmos. 117(D5), doi: 10.1029/2011JD016596.

Ding, X., Zhang, Y.Q., He, Q.F., Yu, Q.Q., Shen, R.Q., Zhang, Y.L., Zhang, Z., Lyu, S.J., Hu, Q.H., Wang, Y.S., Li, L.F., Song, W., and Wang, X.M., 2016. Spatial and seasonal variations of secondary organic aerosol from terpenoids over China. J. Geophys. Res.: Atmos. 121, doi: 10.1002/2016JD025467.

Dockery, D.W., Pope, C.A., Xu, X., Spengler, J.D., Ware, J.H., Fay, M.E., Ferris Jr., B.G., and Speizer, F.E., 1993. An association between air pollution and mortality in six US cities. New Engl. J. Med. 329(24), 1753-1759.

Eddingsaas, N.C., Loza, C.L., Yee, L.D., Chan, M., Schilling, K.A., Chhabra, P.S., Seinfeld J.H., and Wennberg, P.O., 2012. α-pinene photooxidation under controlled chemical conditions-Part 2: SOA yield and composition in low-and high-NO_x environments. Atmos. Chem. Phys. 12(16), 7413-7427.

Forstner, H.J., Flagan, R.C., and Seinfeld, J.H., 1997. Secondary organic aerosol from the photooxidation of aromatic hydrocarbons: Molecular composition. Environ. Sci. Technol. 31(5), 1345-1358.

Goldstein, A.H., Koven, C.D., Heald, C.L., and Fung, I.Y., 2009. Biogenic carbon and anthropogenic pollutants combine to form a cooling haze over the southeastern United States. P. Natl. Acad. Sci. 106(22), 8835-8840.

Guo, H., Jiang, F., Cheng, H.R., Simpson, I.J., Wang, X.M., Ding, A.J., Wang, T.J., Saunders, S.M., Wang, T., Lam, S.H.M., Blake, D.R., Zhang, Y.L., and Xie, M., 2009. Concurrent observations of air pollutants at two sites in the Pearl River Delta and the implication of regional transport. Atmos. Chem. Phys. 9(19), 7343-7360.

Guo, H., Lee, S.C., Louie, P.K., Ho, K.F., 2004. Characterization of hydrocarbons, halocarbons and carbonyls in the atmosphere of Hong Kong. Chemosphere 57(10):1363-72.

Guo, H., Ling, Z.H., Cheung, K., Jiang, F., Wang, D.W., Simpson, I.J., Barletta, B., Meinardi, S., Wang, T.J., Saunders, S.M., and Blake, D.R., 2013. Characterization of photochemical pollution at different elevations in mountainous areas in Hong Kong. Atmos. Chem. Phys. 13(8), 3881-3898.

Guo, H., Ling, Z.H., Simpson, I.J., Blake, D.R., Wang, D.W., 2012b. Observations of isoprene, methacrolein (MAC) and methyl vinyl ketone (MVK) at a mountain site in Hong Kong. J. Geophys. Res.: Atmos. 16;117(D19), doi: 10.1029/2012JD017750.

Guo, H., So, K.L., Simpson, I.J., Barletta, B., Meinardi, S., and Blake, D.R., 2007. C_1-C_8 volatile organic compounds in the atmosphere of Hong Kong: Overview of atmospheric processing and source apportionment. Atmos. Environ. 41(7), 1456-72.

Guo, H., Wang, D.W., Cheung, K., Ling, Z.H., Chan, C.K., and Yao, X.H., 2012a. Observation of aerosol size distribution and new particle formation at a mountain site in subtropical Hong Kong. Atmos. Chem. Phys. 12(20), 9923-9939.

Haddad, I.E., Marchand, N., Temime-Roussel, B., Wortham, H., Piot, C., Besombes, J.L., Baduel, C., Voisin, D., Armengaud, A., and Jaffrezo, J.L., 2011. Insights into the secondary fraction of the organic aerosol in a Mediterranean urban area: Marseille. Atmos. Chem. Phys. 11(5), 2059-2079.

Huang, J.P., Fung, J.C., and Lau, A.K., 2006. Integrated processes analysis and systematic meteorological classification of ozone episodes in Hong Kong. J. Geophys. Res.: Atmos. 111(D20), doi: 10.1029/2005JD007012.

Ho, K.F., Lee, S.C., Guo, H., and Tsai, W.Y., 2004. Seasonal and diurnal variations of volatile organic compounds (VOCs) in the atmosphere of Hong Kong. Sci. Total Environ. 322(1):155-166.

Hu, D., Bian, Q., Li, T.W., Lau, A. K., and Yu, J.Z., 2008. Contributions of isoprene, monoterpenes, β-caryophyllene, and toluene to secondary organic aerosols in Hong Kong during the summer of 2006. J. Geophys. Res.: Atmos. 113(D22), doi: 10.1029/2008JD010437.

Jang, M., Carroll, B., Chandramouli, B., and Kamens, R.M., 2003. Particle growth by acid-catalyzed heterogeneous reactions of organic carbonyls on preexisting aerosols. Environ. Sci. Technol. 37(17), 3828-3837.

Jang, M., Czoschke, N.M., Lee, S., and Kamens, R.M., 2002. Heterogeneous atmospheric aerosol production by acid-catalyzed particle-phase reactions. Science, 298(5594), 814-817.

Janhall, S., Andreae, M.O., and Poschl, U., 2010. Biomass burning aerosol emissions from vegetation fires: particle number and mass emission factors and size distributions. Atmos. chem. Phys. 10(3), 1427-1439.

Kleindienst, T.E., Jaoui, M., Lewandowski, M., Offenberg, J.H., Lewis, C.W., Bhave, P.V., and Edney, E.O., 2007. Estimates of the contributions of biogenic and anthropogenic hydrocarbons to secondary organic aerosol at a southeastern US location. Atmos. Environ. 41(37), 8288-8300.

Kroll, J.H., Ng, N.L., Murphy, S.M., Flagan, R.C., and Seinfeld, J.H., 2006. Secondary organic aerosol formation from isoprene photooxidation. Environ. Sci. Technol. 40(6), 1869-1877.

Lee, S., Kim, H.K., Yan, B., Cobb, C.E., Hennigan, C., Nichols, S., Chamber, M., Edgerton, E.S., Jansen, J.J., Hu, Y., Zheng, M., Weber, R., and Russell, A.G., 2008. Diagnosis of aged prescribed burning plumes impacting an urban area. Environ. Sci. Technol. 42(5), 1438-1444.

Lewandowski, M., Jaoui, M., Offenberg, J.H., Kleindienst, T.E., Edney, E.O., Sheesley, R.J., and Schauer, J.J. (2008). Primary and secondary contributions to ambient PM in the midwestern United States. Environ. Sci. Technol. 42(9), 3303-3309.

Ling, Z.H., Guo, H., Lam, S.H.M., Saunders, S.M., and Wang, T., 2014. Atmospheric photochemical reactivity and ozone production at two sites in Hong Kong: Application of a Master Chemical Mechanism–photochemical box model. J. Geophys. Res.: Atmos. 119(17), 10567-10582.

Maria, S.F., Russell, L.M., Gilles, M.K., and Myneni, S.C., 2004. Organic aerosol growth mechanisms and their climate-forcing implications. Science, 306(5703), 1921-1924.

Offenberg, J.H., Lewandowski, M., Jaoui, M., and Kleindienst, T.E., 2011. Contributions of biogenic and anthropogenic hydrocarbons to secondary organic aerosol during 2006 in Research Triangle Park, NC. Aerosol Air Qual. Res. 11(2), 99-108.

Offenberg, J.H., Lewis, C.W., Lewandowski, M., Jaoui, M., Kleindienst, T.E., and Edney, E.O., 2007. Contributions of toluene and α-pinene to SOA formed in an irradiated toluene/α-pinene/NO x/air mixture: Comparison of results using ^{14}C content and SOA organic tracer methods. Environ. Sci. Technol. 41(11), 3972-3976.

Pope III, C.A., and Dockery, D.W., 2006. Health effects of fine particulate air pollution: lines that connect. J. Air Waste Manage. Assoc. 56(6), 709-742.

562 Reda, A.A., Schnelle-Kreis, J., Orasche, J., Abbaszade, G., Lintelmann, J., Arteaga-Salas, J.M.,
563 Stengel, B., Rade, R., Harndorf, H., Sippula, O., Streibel, T., and Zimmermann, R., 2014. Gas
564 phase carbonyl compounds in ship emissions: Differences between diesel fuel and heavy fuel oil
565 operation. Atmos. Environ. 94, 467-478.
566 Reid, J.S., Koppmann, R., Eck, T.F., and Eleuterio, D.P., 2005. A review of biomass burning
567 emissions part II: intensive physical properties of biomass burning particles. Atmos. Chem. Phys.
568 5(3), 799-825.
569 Rudolph, J., Khedim, A., Koppmann, R., and Bonsang, B., 1995. Field study of the emissions of
570 methyl chloride and other halocarbons from biomass burning in western Africa. J. Atmos. Chem.
571 22(1-2), 67-80.
572 Sippula, O., Stengel, B., Sklorz, M., Streibel, T., Rabe, R., Orasche, J., Lintelmann, J., Michalke,
573 B., Abbaszade, G., Radischat, C., Groger, T., Schnelle-Kreis, J., Harndorf, H., and Zimmermann,
574 R., 2014. Particle emissions from a marine engine: chemical composition and aromatic emission
575 profiles under various operating conditions. Environ. Sci. Technol. 48(19), 11721-11729.
576 So, K.L., and Wang, T., 2003. On the local and regional influence on ground-level ozone
577 concentrations in Hong Kong. Environ. Pollut. 123(2), 307-317.
578 Stocker, T.F., Qin, D., Plattner, G.K., et al. IPCC, 2013: climate change 2013: the physical
579 science basis. Contribution of working group I to the fifth assessment report of the
580 intergovernmental panel on climate change [J]. 2013.
581 Surratt, J.D., Lewandowski, M., Offenberg, J.H., Jaoui, M., Kleindienst, T.E., Edney, E.O., and
582 Seinfeld, J.H., 2007. Effect of acidity on secondary organic aerosol formation from isoprene.
583 Environ. Sci. Technol. 41(15), 5363-5369.
584 Volkamer, R., Jimenez, J.L., San Martini, F., Dzepina, K., Zhang, Q., Salcedo, D., Molina, L.T.,
585 Worsnop, D.R., and Molina, M.J., 2006. Secondary organic aerosol formation from
586 anthropogenic air pollution: Rapid and higher than expected. Geophys. Res. Lett. 33(17), doi:
587 10.1029/2006GL026899.
588 Williams, B.J., Jayne, J.T., Lambe, A.T., Hohaus, T., Kimmel, J.R., Sueper, D., Brooks, W.,
589 Williams, L.R., Trimborn, A.M., Martinez, R.E., Hayes, P.L., Jimenez, J.L., Kreisberg, N.M.,
590 Hering, S.V., Worton, D.R., Goldstein, A.H., and Worsnop, D.R., 2014. The first combined
591 thermal desorption aerosol gas chromatograph-aerosol mass spectrometer (TAG-AMS). Aerosol
592 Sci. Technol. 48(4), 358-370.

Supplementary material for on-line publication only

Click here to download Supplementary material for on-line publication only: Revised supplement material_R.docx